






METHOD ARTICLE

In vitro human stem cell derived cultures to monitor calcium signaling in neuronal development and function [version 1; peer review: 3 approved]

Yojet Sharma ¹, Sankhanil Saha¹, Annu Joseph¹, Harini Krishnan ¹,
Padinjat Raghu ^{1,2}

¹Cellular Organization and Signalling, National Centre for Biological Sciences - TIFR, Bangalore, Karnataka, 560065, India

²Brain Development and Disease Mechanisms, Institute for Stem Cell Science and Regenerative Medicine, Bangalore, Karnataka, 560065, India

v1 First published: 03 Feb 2020, 5:16 (<https://doi.org/10.12688/wellcomeopenres.15626.1>)

Latest published: 03 Feb 2020, 5:16 (<https://doi.org/10.12688/wellcomeopenres.15626.1>)

Abstract


The development of the human brain involves multiple cellular processes including cell division, migration, and dendritic growth. These processes are triggered by developmental cues and lead to interactions of neurons and glial cells to derive the final complex organization of the brain. Developmental cues are transduced into cellular processes through the action of multiple intracellular second messengers including calcium. Calcium signals in cells are shaped by large number of proteins and mutations in several of these have been reported in human patients with brain disorders. However, the manner in which such mutations impact human brain development *in vivo* remains poorly understood. A key limitation in this regard is the need for a model system in which calcium signaling can be studied in neurons of patients with specific brain disorders. Here we describe a protocol to differentiate human neural stem cells into cortical neuronal networks that can be maintained as live cultures up to 120 days in a dish. Our protocol generates a 2D *in vitro* culture that exhibits molecular features of several layers of the human cerebral cortex. Using fluorescence imaging of intracellular calcium levels, we describe the development of neuronal activity as measured by intracellular calcium transients during development *in vitro*. These transients were dependent on the activity of voltage gated calcium channels and were abolished by blocking sodium channel activity. Using transcriptome analysis, we describe the full molecular composition of such cultures following differentiation *in vitro* thus offering an insight into the molecular basis of activity. Our approach will facilitate the understanding of calcium signaling defects during cortical neuron development in patients with specific brain disorders and a mechanistic analysis of these defects using genetic manipulations coupled with cell biological and physiological analysis.

Keywords

Stem cells, neuronal differentiation, calcium imaging, human brain disease, transcriptomics, disease in a dish

Open Peer Review

Reviewer Status 

	Invited Reviewers		
	1	2	3
version 1 03 Feb 2020	 report	 report	 report

- Mohan C. Vemuri**, Thermo Fisher Scientific, Frederick, USA
- Laura N. Borodinsky**, University of California, Davis, Sacramento, USA
- Murali Prakriya**, Northwestern University, Chicago, USA

Any reports and responses or comments on the article can be found at the end of the article.



This article is included in the [Wellcome Trust/DBT India Alliance](#) gateway.

Corresponding author: Padinjat Raghu (praghu@ncbs.res.in)

Author roles: **Sharma Y:** Formal Analysis, Investigation, Methodology, Validation, Visualization, Writing – Original Draft Preparation; **Saha S:** Formal Analysis, Investigation, Methodology, Validation, Visualization, Writing – Original Draft Preparation; **Joseph A:** Formal Analysis, Investigation, Methodology, Validation, Visualization, Writing – Original Draft Preparation; **Krishnan H:** Investigation, Methodology, Software, Visualization, Writing – Original Draft Preparation; **Raghu P:** Conceptualization, Funding Acquisition, Project Administration, Resources, Supervision, Writing – Original Draft Preparation, Writing – Review & Editing

Competing interests: No competing interests were disclosed.

Grant information: This work was supported by the Wellcome Trust through a Wellcome-DBT India Alliance Senior Fellowship to PR [IA/S/14/2/501540]. This work was also supported by the National Centre for Biological Sciences-TIFR, the Department of Biotechnology, Government of India through the Accelerator Program for Discovery in Brain Disorders (BT/PR17316/MED/31/326/2015). AJ was supported by a Research Associate Fellowship from the Department of Biotechnology, Government of India. We thank the NCBS Imaging and NGS facility for support.

The funders had no role in study design, data collection and analysis, decision to publish, or preparation of the manuscript.

Copyright: © 2020 Sharma Y *et al.* This is an open access article distributed under the terms of the [Creative Commons Attribution License](#), which permits unrestricted use, distribution, and reproduction in any medium, provided the original work is properly cited.

How to cite this article: Sharma Y, Saha S, Joseph A *et al.* ***In vitro* human stem cell derived cultures to monitor calcium signaling in neuronal development and function [version 1; peer review: 3 approved]** Wellcome Open Research 2020, 5:16 (<https://doi.org/10.12688/wellcomeopenres.15626.1>)

First published: 03 Feb 2020, 5:16 (<https://doi.org/10.12688/wellcomeopenres.15626.1>)

Introduction

In metazoan development, extracellular cues or signals are sensed and transduced into gene expression programs that lead to cell specification and tissue/organ development. During development, these signals are sensed and transduced into cellular responses through the generation of intracellular second messengers. Changes in intracellular calcium ions $[Ca^{2+}]_i$ are an important mechanism that transduces a large number of signals into cellular behaviors¹ including cell division, migration, shape changes and these are mediated by multiple Ca^{2+} dependent molecular events within cells. Disruption in several elements of these Ca^{2+} dependent processes has been linked to a number of human diseases².

The development of the brain is a complex process wherein epithelial cells that delaminate from the ectoderm form the neural tube, undergo a series of cell divisions, specifications, and movements to give rise to the cell types and organization of the adult brain. Many of these cellular processes are controlled by Ca^{2+} signals which in addition are a key mechanism of neuronal excitability³. As a result, several human brain disorders have been linked to changes in Ca^{2+} signaling in either neurons or glial cells. For example, changes in Ca^{2+} signaling have been linked to a number of human neurodegenerative disorders such as Alzheimer's disease, Huntington disease, and related ataxias and Parkinson's disease⁴. Aberrant Ca^{2+} signaling has also been implicated in the cellular mechanism of severe mental illness such as schizophrenia and bipolar disorder⁵ and disorders of neuronal excitability such as epilepsy⁶. Additionally, spurred by the development of high-throughput next-generation sequencing (NGS) technology, human genetic analyses have described mutations or variants in genes encoding components of the Ca^{2+} signaling toolkit in human patients with brain disorders⁷.

To date, many findings linking human brain diseases to Ca^{2+} signaling have been inferred through the use of immortalized, stable cell lines or cellular models of rodent origin. While these have been hugely influential in driving forward the understanding of human brain disorders, there have been limited studies that have allowed such findings to be corroborated in human brain cells from patients with brain disorders. Conversely, it has been a challenge to test if variations in the DNA sequence of genes encoding components of the Ca^{2+} signaling tool kit in human patients with brain disorders are reflected in Ca^{2+} signaling defects in their brain cells. A principal limitation in obtaining such data is the inability to obtain brain biopsy samples from human patients and subsequently study Ca^{2+} signaling mechanisms using live cell physiology experiments. However, the recent development of methods that allow the generation of induced pluripotent stem cells (iPSC) from somatic tissues of humans and the ability to subsequently differentiate them into neural cell types offers a solution for the need to perform live-cell physiology experiments *in vitro* from neural cells of specific genotypes or specific brain disorders⁸. In this study, we describe protocols to differentiate human neural stem cells into cortical neurons, characterize their molecular properties and perform live cell Ca^{2+} imaging both during neuronal development as well as in mature cultures. The use of this approach will facilitate the analysis

of Ca^{2+} signaling in human cortical neurons *in vitro* and the dissections of Ca^{2+} signaling mechanisms that may underlie the cellular pathogenesis of human brain diseases.

Methods

Materials

A) Neural Stem Cell (NSC) Culture

Equipment

1. Laminar hood, CO_2 incubator to maintain a stable environment of $37^\circ C$, 95% humidity, and 5% CO_2 .
2. Bench-top cell culture centrifuge (Plasto Crafts, Rota 4R V/FA).
3. Tissue culture treated polystyrene dishes.
4. Polystyrene conical tubes.
5. Haemocytometer (Hausser Scientific).
6. Compound phase-contrast light microscope with 4x, 10x and 20x phase objectives.

Stock solutions and reagents

1. Dulbecco's Modified Eagle Medium (Life Technologies, 11995065).
2. Ham's F-12 Nutrient Mix (Life Technologies, 11765054).
3. 50x B-27 serum-free supplement (Life Technologies, 17504044). Aliquots of 1 ml were prepared in 1.5 ml micro-centrifuge tubes and stored at $-20^\circ C$.
4. 50x B-27 supplement minus Vitamin A (Life Technologies, 12587010). Aliquots of 1 ml were prepared in 1.5 ml micro-centrifuge tubes and stored at $-20^\circ C$.
5. FGF-Basic (AA 1-155) Recombinant Human Protein (Thermo Fisher Scientific, PHG0261). It was reconstituted in 5 mM Tris-HCl (pH 7.54) containing 0.1% BSA at a concentration of 100 $\mu g/ml$. Aliquots of 20 μl were made and stored at $-20^\circ C$. A final concentration of 20 ng/ml was used to culture and expand NSCs.
6. Heparin sodium salt (HIMEDIA, CAT NO.: 9041-08-1). Reconstituted according to manufacturer's protocol and aliquots of 20 mg/ml were stored at $4^\circ C$.
7. Penicillin-Streptomycin (P/S) (10,000 U/mL, Life Technologies; 15140122). Aliquots of 10 ml were made and stored at $-20^\circ C$.
8. 100x MEM non-essential amino acids solution (NEAA; Life Technologies; 11140050). Aliquots of 10 ml were made and stored at $4^\circ C$.
9. 100x N-2 supplement (Life Technologies; 17502048). Aliquots of 1 ml were made in 1.5 ml micro-centrifuge tubes and stored at $-20^\circ C$.
10. GlutaMAX™ supplement (Life Technologies; 35050-061). Aliquots of 10 ml were made and stored at $4^\circ C$.
11. StemPro™ Accutase™ Cell Dissociation Reagent (Life Technologies, A1110501).

12. Matrigel, Growth Factor Reduced (Corning, C354277). Aliquots were prepared according to manufacturer's instructions and stored at -80°C.
13. Human recombinant BDNF (Gibco, PHC7074). Reconstituted according to manufacturer's protocol. Aliquots of 10 µl were stored at -20°C. A final concentration of 10 ng/ml was used during neuronal differentiation.
14. Human recombinant GDNF (Gibco, PHC7045). Reconstituted according to manufacturer's protocol. Aliquots of 10 µl were stored at -20°C. A final concentration of 10ng/ml was used during neuronal differentiation.
15. Human recombinant IGF-1 (Gibco, PHG0078). Reconstituted according to manufacturer's protocol. Aliquots of 10 µl were stored at -20°C. A final concentration of 10 ng/ml was used during neuronal differentiation.
16. N-[(3,5-Difluorophenyl) acetyl]-L-alanyl-2-phenyl]glycine-1,1-dimethylethyl ester (DAPT)—γ-secretase inhibitor (Sigma-Aldrich, D5942-5MG). It was reconstituted in DMSO at a concentration of 5 mM. Aliquots of 50 µl were stored at -20°C. A final concentration of 2 µM was used during neuronal differentiation.
17. L- Ascorbic acid 2-phosphate sesquimagnesium salt hydrate (Sigma-Aldrich, A8960). Reconstituted in sterile water to make a stock solution of 5 mg/mL, filter-sterilized and stored at -20°C.
18. Poly-L-ornithine (PLO) 0.01% (Sigma-Aldrich, P4957).
19. Laminin (LN) (Gibco, 23017015, 1 mg/ml solution).
20. PSC Cryomix freezing mixture (Thermo Fisher Scientific, A2644601). Aliquots were prepared of 10 ml and stored at -20°C.

Primary antibodies

Table 1. List of primary antibodies used in this study.

Primary antibodies	Source	Company	Catalog number	Dilution	RRID
Nestin (10C2)	Mouse (monoclonal)	Thermo Fisher	MA1-110	1:50	AB_2536821
SOX1	Rabbit (polyclonal)	Abcam	ab87775	1:200	AB_2616563
SOX2 (20G5)	Rabbit (monoclonal)	Abcam	ab92494	1:100	AB_10585428
Ki67 [B126.1]	Mouse (monoclonal)	Abcam	ab8191	1:100	AB_306346
Doublecortin	Rabbit (polyclonal)	Abcam	ab18723	1:500	AB_732011
Beta 3 Tubulin	Mouse (monoclonal)	Abcam	ab78078	1:400	AB_2256751
CTIP2 [25B6]	Rat (monoclonal)	Abcam	ab18465	1:800	AB_2064130
MAP2	Chicken (polyclonal)	Abcam	ab5392	1:1000	AB_2138153
Neurofilament	Chicken (polyclonal)	Abcam	ab4680	1:500	AB_304560
GFAP	Chicken (polyclonal)	Abcam	ab4674	1:1000	AB_304558
OLIG2 (1G11)	Mouse (monoclonal)	Thermo Fisher	MA5-15810	1:200	AB_11152534
Synapsin I	Rabbit (polyclonal)	Abcam	ab64581	1:200	AB_1281135
Synaptophysin	Rabbit (polyclonal)	Abcam	ab32594	1:500	AB_778204

Table 2. List of secondary antibodies used in this study.

Secondary antibodies	Species	Company	Catalog number	Dilution
Alexa 488	Goat α-Mouse IgG (Polyclonal)	Life Technology	A11001	1:300
Alexa 568	Goat α-Chicken IgG (Polyclonal)	Life Technology	A11041	1:300
Alexa 568	Donkey α-Rabbit IgG (Polyclonal)	Life Technology	A10042	1:300
Alexa 568	Goat α-Rat IgG (Polyclonal)	Life Technology	A11077	1:300
Alexa 633	Goat anti-chicken IgG (Polyclonal)	Life Technology	A21103	1:300
Alexa 633	Goat α-Rabbit IgG (Polyclonal)	Life Technology	A21070	1:300

B) MediumNeuronal Expansion Medium (NEM):

- a) Dulbecco's Modified Eagle Medium/Nutrient Mixture F-12 (DMEM/F-12, 1:1 ratio)
- b) 1x B27 Supplement minus vitamin A
- c) 1x N2
- d) 1x NEAA
- e) 1x GlutaMAX
- f) 100 U/ml Penicillin-Streptomycin
- g) 20 ng/ml bFGF
- h) 2 µg/ml Heparin Sulfate

The medium can be stored at 4°C for up to 2 weeks.

Neuronal Differentiation Medium (NDM):

- a) Dulbecco's Modified Eagle Medium/Nutrient Mixture F-12 (DMEM/F12, 1:1 ratio)
- b) 1x B27 Supplement (with vitamin)
- c) 1x N2
- d) 1x NEAA
- e) 1x GlutaMAX
- f) 100 U/ml Penicillin-Streptomycin
- g) 10 ng/ml BDNF
- h) 10 ng/ml GDNF
- i) 10 ng/ml IGF-1
- j) 2 µM DAPT

The medium can be stored at 4°C for up to 2 weeks.

C) Calcium imaging*Equipment*

1. Wide-field fluorescence microscope Olympus IX-83.
2. [CellSens Dimensions software](#) (Olympus, build 16686) with the necessary modules for region of interest (ROI), background subtraction, time-lapse imaging and intensity measurement.
3. 35mm glass bottom dishes prepared using in-house institute facility.

Solutions

1. Poly-L-ornithine, 0.01%. This was the same concentration used for the coating glass-bottom dishes.
2. Laminin (1 mg/ml). A final concentration of 10–15 µg/ml was used for coating glass-bottom dishes. The stocks were prepared as per the manufacturer's instructions.

3. Fluo-4 AM (1 mM, Molecular probes, F14201). A final concentration of 4 µM was used for calcium imaging experiments.
4. Fura-2 AM (Thermo Fisher Scientific, F-1221). A final concentration of 4 µM was used for the store operated calcium entry (SOCE) imaging experiments.
5. TTX (HelloBio, CAS:18660-81-6). A final concentration of 10 µM was used. Working stock was prepared according to the manufacturer's instructions.
6. Nimodipine (Sigma, N149). A final concentration of 10 µM was used. 50 mM working stock was prepared by reconstituting in methanol.
7. Ionomycin salt (Calbiochem, 407952-10MG). A 10 mM main stock of the salt was prepared by dissolving in DMSO. A final concentration of 20 µM was used for calcium imaging experiments, during calibration.
8. Pluronic acid, PF-127 (Sigma, CAS:9003-11-6, P2443-250G). A final concentration of 0.002% was used.
9. Hanks Balanced Salt Solution (HBSS): 10 mM Glucose, 10 mM HEPES, 118 mM NaCl, 4.96 mM KCl, 1.18 mM MgSO₄, 1.18 mM KH₂PO₄, 2 mM CaCl₂; pH-7.4 stored at 4°C.
10. Ethylene glycol-bis(2-aminoethylether)-*N,N,N',N'*-tetraacetic acid (EGTA, Sigma, E3889). A stock solution of 100 mM was made and stored at room temperature. A final concentration of 4 mM was used for the SOCE experiments.

Methods**A. Maintenance and expansion of XCL1 Neural Stem Cells (NSCs)**

1. XCL1 NSCs (XCell Science Inc.; Novato, CA, USA; passages 7–17) was used for our experiments.
2. They were plated and expanded in NEM on 6-well plates coated with Matrigel for 1 h at 37°C/ 5% CO₂.
3. The NSCs were routinely split in 1:3 ratio and expanded in a manner so that the cells could be utilized for experiments described in this manuscript.
4. During expansion process, the cultures were checked for mycoplasma. Following this, they were cryopreserved.

B. Cryopreservation of XCL1 NSCs

Frozen stocks of XCL1 NSCs were prepared by freezing of cells (~1×10⁶) in 1.5 ml PSC Cryomix.

C. Differentiation of NSCs into cortical neurons

1. NSCs (0.1–0.2 × 10⁶ cells) were plated on sterile 35mm glass bottom dishes.
2. These glass bottom coverslips were coated with poly-L-ornithine for 1 h at 37°C/ 5% CO₂.

- Coverslips were dried for 30 min. Subsequently, 10–15 µg/ml Laminin was used for a 2nd coating and incubated for 1 h at 37°C/ 5% CO₂.
- The NSCs were allowed to adhere and reach 70% confluency in NEM for 1–2 days.
- Then, NEM was withdrawn from the 35mm dishes and gently replaced with neural differentiation medium (DMEM/F12, 1X N2, 1X B27 with vitamin A, non-essential amino acids, 10 ng/ml BDNF, 10 ng/ml GDNF, 10 ng/ml IGF-1, 200 µM ascorbic acid, penicillin/streptomycin).
- Cultures were fully refreshed with medium every 2 days during DAPT treatment (i.e. 2 weeks).
- After 4 weeks, cultures were fully refreshed with medium every 3–4 days. ICC and calcium imaging was performed between 7 and 60 days after plating NSCs.

D. Karyotyping of NSCs

NSCs were grown to approximately 70% confluency in a 35 mm dish (cultured as mentioned above) and then sent to a NABL (National Accreditation Board for Testing and Calibration Laboratories-India) certified laboratory for karyotype analysis.

E. Calculation of cell proliferation rate

- NSCs were seeded on a 24 well plate, 5000 cells per well, three replicates for each day.
- Cells from 3 wells were collected every 24 hours and number of cells from each well were counted using haemocytometer. This was repeated for 7 days.

F. Characterization of NSCs and neurons by immunofluorescent staining

- Cell cultures were fixed using 4% formaldehyde in phosphate-buffered saline (PBS) for 20 min and permeabilized with 0.1% TX 100 for 5 min, and incubated at room temperature for 1hr in a blocking solution of 5% BSA in PBS.
- Primary antibodies were incubated overnight at 4°C in blocking solution, followed by incubation with secondary antibodies in blocking solution (Invitrogen) for 1 hour.
- Confocal images were recorded by collecting a range of z-stack using an Olympus FV 3000 confocal microscope. The image stack was merged using Z-project (maximum intensity projection) tool using ImageJ 1.52n (National Institute of Health, USA, <http://imagej.nih.gov/ij>).

G. Characterization of neurons by post-hoc immunofluorescent staining

- Post-calcium imaging, neurons were washed thrice for 10 min with HBSS buffer to wash out calcium imaging dye.

- Neurons were fixed with either 4% PFA dissolved in PBS for 20 min or with ice-cold methanol for 5 min on bench and washed twice with PBS for 5 min each.
- 0.1% Triton-X dissolved in PBS was used to permeabilize cells for 5 min.
- 5% BSA or 10% Normal Goat Serum (NGS) was used for blocking for 1 hr at room temperature. BSA and NGS were dissolved in PBS.
- Primary antibodies were used at the dilution mentioned in [Table 1](#) and were diluted in either 5% BSA or 10% NGS. The cells were incubated with primary antibodies overnight at 4°C.
- Following washes with PBS, secondary antibodies ([Table 2](#)) were used at 1:300 dilution in PBS+ 5% BSA or 10% NGS and DAPI was used as a nuclear marker at a dilution of 1:1000.

H. Quantitative real-time PCR

Isolation of RNA and synthesis of cDNA:

- Total RNA was isolated from cells in culture at specified ages using TRIzol (Ambion, Life Technologies, catalog no. 15596018) as per manufacturer's instructions.
- The total RNA was quantified using a Nanodrop 1000 spectrophotometer (Thermo Fisher Scientific). Three biological replicates for isolated RNA from each sample were used for the validation of gene expression by quantitative real time PCR (qRT-PCR).
- Approximately 1 µg of total RNA was used per sample for cDNA synthesis.
- The RNA was treated with 1U of DNase I (amplification grade, Thermo Fisher Scientific, catalog no. 18068-015) in a reaction mixture of 45.5 µl containing 10 mM DTT and 40U of RNase inhibitor (RNaseOUT, Thermo Fisher Scientific, catalog no.10777-019). The reaction mixture was incubated at 37°C for 30 min followed by heat inactivation at 70°C for 10 min.
- For the synthesis of cDNA, 200U of Superscript II Reverse Transcriptase (Invitrogen, catalog no. 18064-014) was added to the reaction along with 2.5 µM random hexamers, and 0.5 mM dNTPs in a final volume of 50 µl. The reaction mixture was incubated at 25°C for 10 min, followed by 42°C for 60 min and heat inactivated at 70°C for 10 min (ProFlex PCR Systems, Life Technologies).

qRT-PCR analysis:

- Quantitative qRT-PCR analysis was performed in a total volume of 10 µl with Power SYBR Green Master mix (Applied Biosystems, catalog no.4367659) on an Applied Biosystems ViiA7 system.

7. qRT-PCR analysis was performed with diluted cDNA samples and primers for genes of interest and GAPDH was used as an internal control. The primers used for qRT-PCR were designed using [Primer-BLAST](#), NCBI and their details are provided in [Table 3](#).
8. Technical triplicates were performed for each qRT-PCR reaction. As a control, a reaction with no reverse transcriptase was also set up.
9. The reaction was run using the following conditions: 50°C for 2 minutes, 95°C for 10 minutes, followed by 40 cycles of 95°C for 30 seconds (denaturation), 60°C for 30 seconds (annealing) and 72°C for 45 seconds (extension).
10. A dissociation curve was generated after amplification to distinguish the actual PCR products from primer dimers and non-specific products under the following conditions: 95°C for 15 seconds, 60°C for 1 minute, 95°C for 30 seconds and 60°C for 15 seconds.
11. The C_t values obtained for different genes were normalized to those of GAPDH from the same sample. The relative expression levels were calculated using ΔC_t method, using the formula $2^{-\Delta C_t}$.
12. One-way ANOVA was used for Statistical analysis using [GraphPad Prism 5.0](#) software, and $p < 0.05$ was considered significant.

Table 3. List of qRT-PCR primers.

Gene name	NCBI Reference (mRNA)	Forward primer (5'-3')	Reverse primer (5'-3')
<i>GAPDH</i>	NM_002046.6	TGCACCACCAACTGCTTAGC	GGCATGGACTGTGGTCATGAG
<i>CTIP2/BCL11B</i>	NM_138576.3	CAGGAGAACATTGCAGGGCCG	GGCACGCAGAGGTGAAGTGA
<i>CUX1</i>	NM_181552.3	TGCAGAAAACCTGCAGAGCCG	TTTAAGGCAGGGTCGAGGGC
<i>DCX</i>	NM_000555.3	TGACTCAGCAAACGGAACCT	CGAGTCCGAGTCATCCAAGG
<i>GAD67/GAD1</i>	NM_000817.2	AAGCTACACAAGGTGGCTCC	CATCCGGAAGAAGTTGGCCT
<i>GFAP</i>	NM_002055.4	AGAACCGGATCACCATTCCC	CACGGTCTTCACCACGATGT
<i>MAP2</i>	NM_002374.3	GCGCCAATGGATTCCCATAC	CAGACACCTCCTCTGCTGTT
<i>NEFH</i>	NM_021076.3	GGCACTGAAAAGCACCAAGG	CTGCTGAATGGCTTCCTGGTA
<i>NEUN/RBFOX3</i>	NM_001082575.2	ACGATCGTAGAGGGACGGAA	TTAGCTTCCAGCCGTTGGT
<i>OLIG2</i>	NM_005806.3	GGTGCGCAAGCTTCCAAGA	GATCTCGCTCACCAGTCGCT
<i>PSD95/DLG4</i>	NM_001365.4	GAGAGTCAGAAATACCGCTACC	CCCGTTCACCTGCAACTCAT
<i>SYN</i>	NM_006950.3	GTGGACACGTGCTCAGAGAT	AGGAACCCACCACCTCAATG
<i>SYP</i>	NM_003179.2	TGGGGACTACTCCTCGTCAG	GTGGCCAGAAAAGTCCAGCAT
<i>TUBB3</i>	NM_001197181.1	ATCTTTGGTCAGAGTGGGGC	CTGCAGGCAGTCGCAGTTTT
<i>VGLUT1/SLC17A7</i>	NM_020309.3	AGCTGGGATCCAGAGACTGT	CCGAAAACCTCTGTTGGCTGC
<i>GLS</i>	NM_014905.4	GCTATGGACATGGAACAGCG	TATTCCACCTGTCTTGGGGA
<i>SATB2</i>	NM_001172509.1	AAGGCCGTGGGAGGTTTGAT	TTCCGCACCAGGACAAACT
<i>STIM1</i>	NM_001277961.1	CCTGTGGAAGGCATGGAAGT	GTCCCTGTCATGGTGGTGT
<i>STIM2</i>	NM_001169118.1	GCATGTCACTGAGTCCACCA	TCTCTGTGCAGATGGCTGTG
<i>ORAI1</i>	NM_032790.3	GGTCAAGTTCTTGCCCTCA	CGTTGAGCTCCTGGAAGTGT
<i>ORAI2</i>	NM_001126340.3	ATCCACTTCTACCGCTCCCT	CATCTGACAAATCCCCGCCT
<i>ORAI3</i>	NM_152288.3	AGAGTGACCACGAGTACCCA	TGTGGATGTTGCTCACAGCT
<i>ITPR1</i>	NM_001099952.2	TGCCAAAAGCAGTTCTGGA	TACGGTCCCCAGCAATTTCC
<i>ITPR2</i>	NM_002223.4	CTGAGAAGCGAGGGTGACAA	CCAGCTGGTGTGCAATTGA
<i>ITPR3</i>	NM_002224.4	GTTCTGACGTGTGACGAGT	AAGCGGTACAAGCCATTCCA
<i>ATP2A2/SERCA2</i>	NM_001681.4	GCAATTGTGGGTGTATGGCA	ATCCGCTGCACACTCTTTCT
<i>ATP2A3/SERCA3</i>	NM_005173.4	TCGAGGCCCTGAAGGAGTAT	CAGCGTGGTGGACTTGATCT

I. Calcium imaging to measure transients

Cell preparation and dye loading:

1. 35mm glass-bottom coverslip dishes were UV sterilized and coated with PLO/Laminin before plating cells. 0.01% PLO was coated for 1hr followed by Laminin coating. Following each coating step, the dishes were air-dried.
2. 0.1–0.2 million cells were seeded in 35mm glass-bottom coverslip dishes. Prior to imaging, NDM was aspirated out of the dishes and the cells were washed twice (each for 5 min) with HBSS (10 mM HEPES, 118 mM NaCl, 4.96 mM KCl, 1.18 mM MgSO₄, 1.18 mM KH₂PO₄, 2 mM CaCl₂; pH-7.4), supplemented with 10 mM Glucose.
3. Calcium imaging was carried out on 7, 14, 21, 30 and 45 days *in-vitro* (DIV) neurons. Prior to dye loading, 1mM of Fluo-4/AM was diluted to 4 μM in calcium imaging buffer; to avoid compartmentalization of the dye, PF-127, a permeabilizing agent, was diluted to 0.002% in the calcium imaging buffer.
4. Cells were incubated for 30-45 mins in dark at room temperature with 4 μM Fluo-4 AM.
5. Following dye loading, the cells were washed again with the calcium imaging buffer thrice, each wash for 5 mins. Finally, cells were incubated for an additional 20 min at room temperature to facilitate de-esterification.

Imaging:

6. The imaging parameters were set before initiating imaging. Ca²⁺ imaging was performed for 10 min with a time interval of 1second using a 20X objective of wide-field fluorescence microscope Olympus IX-83.
7. A four-minute long baseline measurement was recorded to visualize calcium transients, followed by the addition of TTX to abolish calcium transients for another 4 mins.
8. Lastly, ionomycin was added to the dish followed by 5 mM MnCl₂ solution for calibration.

Image analysis:

9. Image analysis was performed using the CellSens Dimensions; a region of interest (ROI) was drawn manually around each cell and the time-lapse acquisition mode of the software was used to track fluorescence changes over time.
10. The raw fluorescence intensity values from each neurons was normalized to the first fluorescence intensity signal of the baseline recording.
11. A first-derivative filter was then used to threshold and identify calcium transients.
12. A calcium event for our experiments was defined by a positive derivative value of 2×SD + average of normalized intensity in regions where devoid of transients.

13. Number of spikes and amplitude from individual neurons were measured manually from first-derivative filter traces.

14. The analyses were plotted on Graph Pad Prism 7.

J. Calcium imaging for SOCE experiments

Dye loading:

1. The NSCs and the neurons were grown on Poly-L-Lysine (PLL)/ Laminin coated coverslip dishes (as described before).
2. Prior to imaging, the cells were washed twice with HBSS (10 mM HEPES, 118 mM NaCl, 4.96 mM KCl, 1.18 mM MgSO₄, 1.18 mM KH₂PO₄, 2 mM CaCl₂; pH-7.4), supplemented with 10 mM Glucose.
3. The cells were then loaded with 4 μM of the dual-excitation single emission ratiometric Ca²⁺ indicator Fura-2 AM (Acetoxymethylester, Invitrogen) and incubated in dark at room temperature for 30 min. Fura-2 AM was dissolved in the HBSS buffer, containing 0.002% Pluronic F-127.
4. After the loading, excess dye was washed off by washing the cells thrice with HBSS and cells were incubated for an additional 20 min at room temperature before imaging for de-esterification.
5. Just before imaging, HBSS buffer was replaced by 'zero Ca²⁺ HBSS' (10 mM HEPES, 118 mM NaCl, 4.96 mM KCl, 1.18 mM MgSO₄, 1.18 mM KH₂PO₄, 10 mM Glucose; pH-7.4).

Imaging:

6. Ca²⁺ imaging was performed for 17 min using a 40X objective (N.A. 0.75) of wide-field fluorescence microscope Olympus IX-83.
7. The cells were alternately illuminated at 340 nm and 380 nm using band-pass filters and the fluorescence emission at 510 nm was acquired using an EM-CCD camera (Evolve 512 Delta, Photometrics). 340 nm/380 nm ratio images were recorded at every 5 s intervals.
8. Basal cytosolic Ca²⁺ was recorded in 'zero Ca²⁺ HBSS' for 12 frames.
9. Following this, 10 μM Thapsigargin (TG, Invitrogen) was added to the cells for inducing Ca²⁺ release from the endoplasmic reticulum store; images were acquired every 5 s for 84 frames.
10. 2 mM CaCl₂ was added to the extracellular buffer to induce SOCE after which images were recorded every 5 s for 60 frames.
11. Finally, 20 μM Ionomycin (Calbiochem) was added and 24 frames were recorded for obtaining the maximum fluorescence intensity.
12. Subsequently, 4 mM EGTA (containing 0.01% Triton-X-100) was added for chelating all the cytosolic

Ca²⁺ and 24 frames were recorded for the minimum fluorescence intensity for each cell.

Image analysis:

- Image analysis was performed using the CellSens Olympus software; a region of interest (ROI) was drawn manually around each cell and the time-lapse acquisition mode of the software was used to track fluorescence changes over time.

The emission intensities corresponding to 340 nm and 380 nm excitations were used to calculate the 340/380 ratio for each cell across all time points. The [Ca²⁺]_i was estimated using the Grynkiewicz equation⁹ as follows:

$$[Ca^{2+}]_{nM} = K_d \times SF \times \left(\frac{R - R_{min}}{R_{max} - R} \right)$$

where R_{min} and R_{max} correspond to the minimum 340/380 ratio and maximum 340/380 ratio respectively. 225 nM was taken as K_d for Fura-2 in human cells and SF (scaling factor) was calculated for each cell by dividing the fluorescence emission intensity at Ca²⁺ free form with the fluorescence emission intensity at Ca²⁺ bound form of the dye after excitation at 380 nm.

K. Library preparation, sequencing and RNA-Seq data analysis

Library preparation:

- Total RNA was isolated from XCL1 NSCs, 45 DIV and 60 DIV neurons using TRIzol as per manufacturer's instructions.
- Total RNA was quantified using Qubit4 dsDNA HS Assay Kit (Thermo Fisher Scientific, catalog no.Q32854) and run on a Bio-analyzer chip (Agilent High Sensitivity DNA Chip, catalog no.5067-4626) for ensuring the integrity.
- Approximately 150 ng of total RNA (RIN values > 9) was used per sample to prepare libraries using the NEBNext Ultra II Directional RNA Library Prep Kit for Illumina (New England Biolabs, catalog no. E7760L) following the NEB Next Poly(A) mRNA Magnetic Isolation Module (catalog no.E74906).
- The prepared libraries were then run on a Bio-analyzer using Agilent High Sensitivity DNA Chip to check their size.
- The libraries were then quantified by qRT-PCR and sequenced on Illumina HiSeq 2500 sequencing platform using 2x100 bp sequencing format (Illumina).
- Biological triplicates were performed for RNA isolated from XCL1 NSCs while duplicates were performed for RNA isolated from 45 DIV and 60 DIV neurons. All the seven samples were run in a 2X100 paired end Single Flow Cell.

Differential expression of genes:

- The paired-end reads (50 million reads per sample), quality checked and processed (adapter removal and trimming) were obtained from RNA sequencing as mentioned above.
- The quality of the reads was further verified using FastQC v0.11.8¹⁰ quality check.
- The fasta sequence file and .gtf file for human genome were downloaded from the Ensemble database.
- The reads were aligned to the human genome. The reads for each sample (NSC in triplicate, 45 DIV and 60 DIV neurons in duplicates) were mapped on the human genome (Genome Reference Consortium Human Build 38 Organism: *Homo sapiens* (human)).
- RSEM v1.3.1¹¹ was used for preparing the reference files and for mapping the reads. The reads were mapped to the reference genome and a count file containing counts of reads for each gene was obtained using rsem-calculate-expression module.
- The DESeq 1.38.0¹² method was used for calculating the log₂ fold change (log₂FC) from the counts for each gene.
- The genes with a log₂FC of +1.5 and greater and significant p-value and FDR (<0.05 and <0.05 respectively) were considered to be upregulated while the genes with a log₂FC of -1.5 and lesser with significant p-value and FDR (<0.05 and <0.05 respectively) were considered to be downregulated.
- A list of genes involved in calcium signalling in neurons was collated from¹³. A total of 109 genes were selected to understand the variation in calcium signalling between NSCs and DIV45 and DIV60 neuron samples. The differential expression of these genes based on their log₂FC values was analysed and represented in the form of heatmap.

Results

Characterization of NSC

We characterized the starting culture of NSC using a number of approaches. The cell line that we used, XCL-1 was originally derived from CD34+ cord blood cells of a normal newborn male subject. Although purchased commercially, we karyotyped them during this study and found them to have normal karyotype (Figure 1A); karyotyping was repeated every 10 passages. XCL-1 NSCs were cultured on a plastic surface coated with a commercially available extracellular matrix (Matrigel-Corning). They attached readily to this substratum and had a doubling time of ca. 24 hrs (Figure 1B). Ki-67, a proliferative marker, was also used to validate the proliferation of NSCs (Figure 1C vii, ix) and we observed 32.15% of cells positive for Ki-67 (91 out of 283 cells were positive for Ki-67). Immunocytochemistry analysis showed that these NSCs expressed the widely used NSC markers, Nestin, SOX1, and SOX2 (Figure 1 C i-vi). For example, in the case of Nestin, 98% of the cells in the culture showed expression of this protein marker.

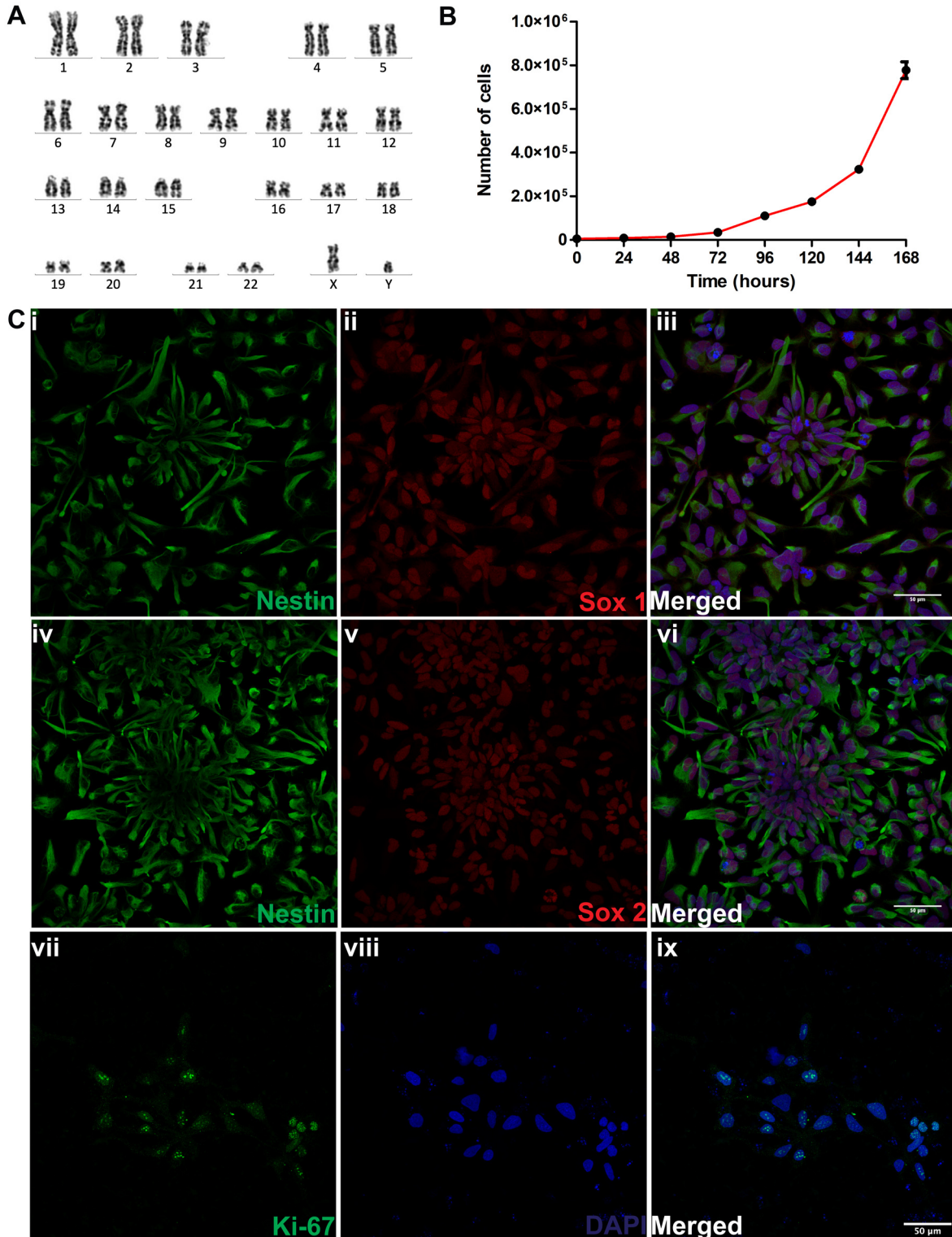


Figure 1. Characterization of XCL-1 neural stem cells (NSCs). (A) Cytogenetic characterization of NSCs by karyotyping. Image of chromosome from a metaphase spread of XCL1 showing normal number and banding pattern of each of the 22 pairs of autosomes, X and Y chromosomes. (B) Proliferation curve of XCL1, with the values represented as mean \pm SEM of 3 independent measurements. Y-axis depicts the number of cells and the X-axis, age in hours (C) Confocal images of XCL-1 showing the expression of (i–iii) Nestin/SOX1. Confocal images of (iv–vi) Nestin/SOX2 and (vii–ix) Ki-67/DAPI. The NSCs were regularly observed in their typical neural rosette morphology. The confocal images in this panel were brightness adjusted using ImageJ for better visualization. Scale bar 50 μ m.

Differentiation of NSC into neurons *in vitro*

We obtained human neuronal cultures *in vitro* by differentiating NSCs. The NSCs were expanded and re-plated on PLO-laminin coated coverslip dishes in Neural Expansion Medium. The neuronal differentiation protocol has been outlined in Figure 2A. Initiation of cortical neuronal patterning is achieved by gradually withdrawing bFGF and heparin and addition of neurotrophic factors BDNF, GDNF, IGF-1 and the γ -secretase inhibitor DAPT that inhibits Notch signaling. Over 7 days *in vitro* (DIV), the NSCs began to exhibit reduced proliferation and also show cell death (Figure 2Bi-vi). They also form small aggregates and established elongated spindle processes. Such cultures were maintained for upto a maximum of 120 DIV and characterized for the expression of transcripts and proteins to establish the molecular process of neuronal differentiation and the identity of the cells in culture.

The differentiation of NSC into cortical neurons follows a number of stages including early neuronal differentiation, the formation of neurons typical of each of the six layers of the human cerebral cortex and the development of synaptic connections. We monitored these events by measuring the expression of transcripts for genes known to be expressed at each of these stages of development. Gene expression analysis was done using qRT-PCR on neuronal cultures at 7, 14, 21, 30, 45 and 60 DIV. This analysis revealed a gene expression pattern consistent with the known steps of cortical neuronal differentiation. We found that the expression of the immature neuronal marker β 3-tubulin (TUBB3) starts increasing from 7 DIV onwards (Figure 3A). Doublecortin (DCX), a microtubule binding protein required for migration of neural progenitors and associated with X-linked lissencephaly in humans^{14,15} increased over the first 21 DIV after which its transcripts declined (Figure 3B). The decline in DCX expression at DIV21 was associated with a continued increase in the expression of the mature neuronal marker NeuN (Figure 3E) that is encoded by *RBFOX3*, a member of the Foxo family of transcription factors; this is consistent with the previously reported expression pattern of NeuN *in vivo*¹⁶. In addition, we found that

expression of the mature neuronal markers microtubule-associated protein 2 (*MAP2*) and Neuronal Heavy polypeptide (*NEFH*) shows delayed temporal expression compared to β 3-tubulin transcripts (Figure 3D, E). A parallel immunocytochemistry study revealed that TUBB3 increases progressively from 21 DIV onwards (Figure 3F i, vi, xi, xvi). By contrast, although expression of the NEFH protein was detected from 21 DIV, enhanced expression was only seen by 60 DIV (Figure 3F xvii); this was also true for MAP2 (Figure 3F xviii).

Development of human cortical layer cell types

The development of the human cerebral cortex is choreographed through the expression of unique transcription factors typical of and necessary for specific layers of the developing cortex. To test the extent to which our *in vitro* cultures recapitulate the cell types in these cortical layers, we measured the expression of these transcription factors during *in vitro* development. Cut like homeobox 1 (*CUX1*) is a transcription factor expressed in and required for dendritic morphogenesis in Layer II-III cortical neurons¹⁷. We found that the expression of *CUX1* progressively rose from 7 DIV to 21 DIV after which it remained elevated (Figure 4B). Likewise, the expression of *CTIP2* a transcription factor typical of layers V-VI was upregulated at 21 DIV and remained elevated thereafter (Figure 4A). Immunolabelling with a CTIP2 antibody revealed the expression of CTIP2 protein in the nucleus of a subset of neurons in our 21 DIV and 60 DIV cultures (Figure 4 D,E). We also quantified the expression of *SATB2*, a chromatin remodeling factor that regulates the specification of neurons in cortical layer II-IV^{18,19} and found that its expression is upregulated from 21 DIV onwards and then increased progressively (Figure 4C). Thus, our *in vitro* differentiation protocol recapitulates key molecular markers of human cerebral cortex neurogenesis as previously reported *in vivo*.

Expression of synaptic transmission elements *in vitro*

We also measured the expression of transcripts for key proteins involved in the organization and function of the synapse. These include the presynaptic protein synapsin (*SYN*) synaptophysin

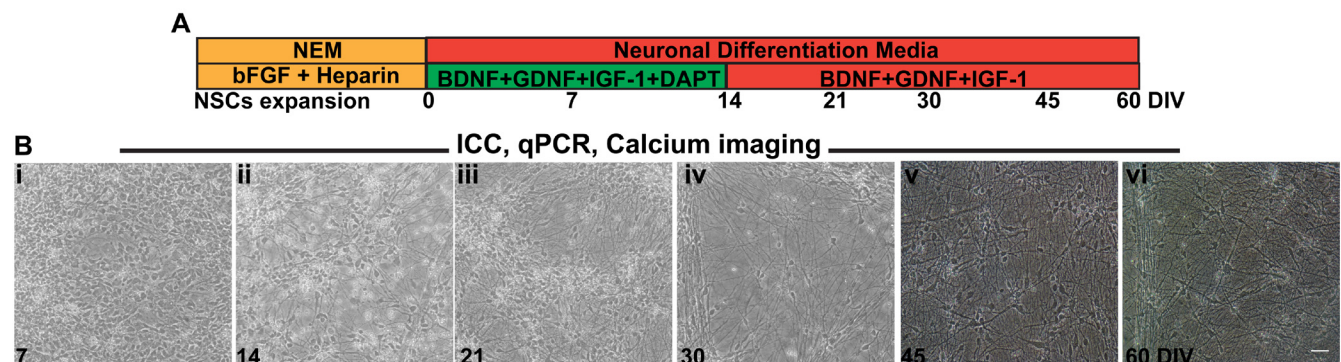


Figure 2. Neuronal differentiation of XCL-1 neural stem cells (NSCs). (A) Schematic representation of neuronal maintenance and differentiation. Top row shows the name of the medium and the bottom row indicates the growth factors and other small molecules added in each case. The age of the cultures is shown below in days *in vitro* (DIV). (B) Phase contrast images of NSC and cultures during differentiation. At each time point, cells were characterized using immunocytochemical staining (ICC), qRT-PCR, and calcium imaging. (i) 7 DIV (ii) 14 DIV (iii) 21 DIV (iv) 30 DIV (v) 45 DIV and (vi) 60 DIV. Some cell death was observed in 7 DIV which gradually decreased over days in culture; (ii) By 14 DIV, bipolar neuronal morphologies are observed (iii-vi) From 21 DIV- 60 DIV cells start to cluster together in clumps and spread out as a mat. Scale bar 50 μ m.

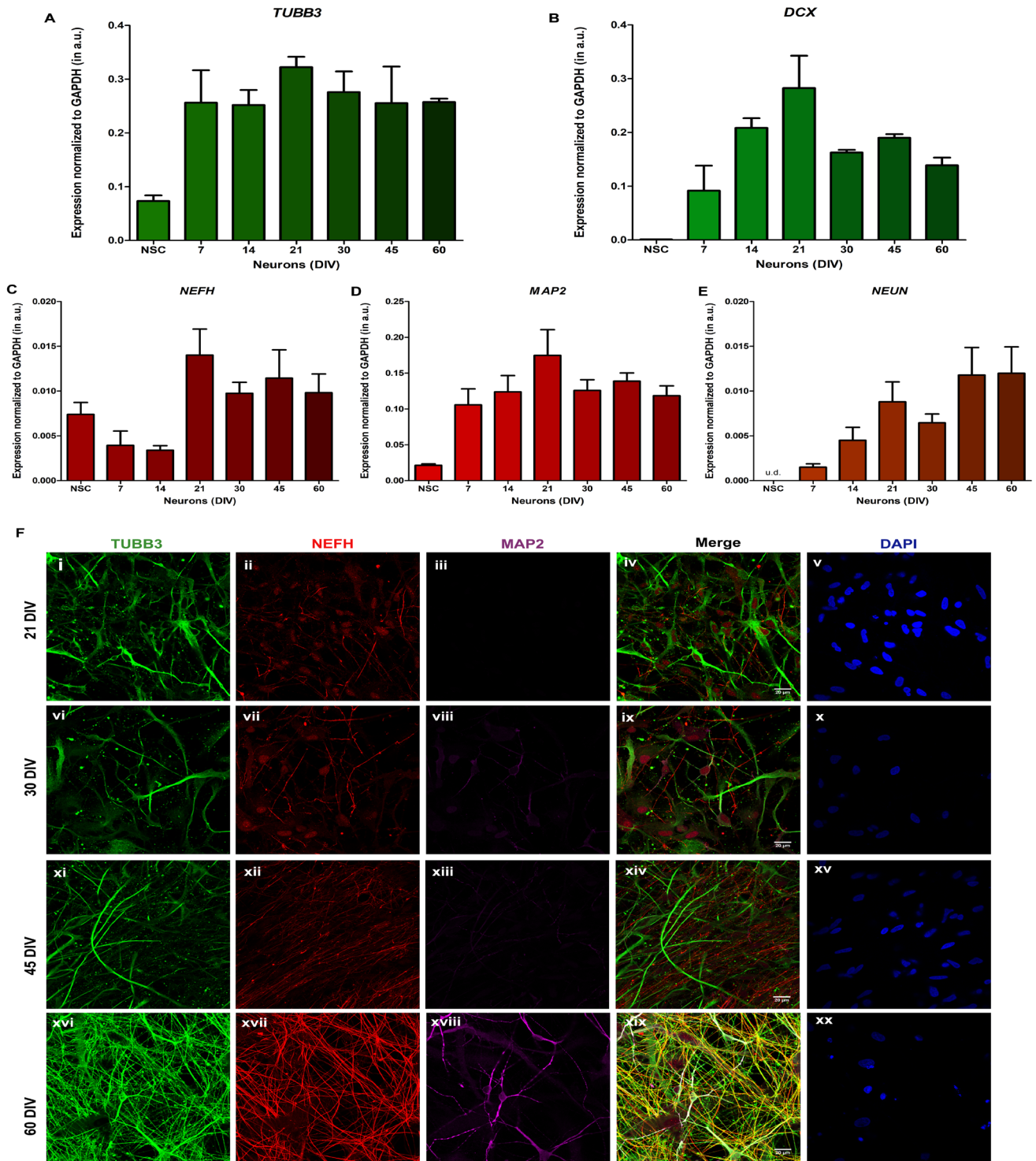


Figure 3. Characterization of neurons differentiating from neural stem cells. (A) to (E) Relative mRNA expression levels of early and late neuronal markers at stages of neuronal differentiation obtained from qRT-PCR. The figures A and B illustrate the relative expression of early neuronal markers *TUBB3* and *DCX*, and figures C, D and E shows *NEFH*, *MAP2* and *NEUN* respectively. X-axis shows the age of the cultures in days *in vitro* (DIV). The expression levels of each transcript have been normalized with *GAPDH* as endogenous control and the values represented in the terms of $2^{-\Delta Ct}$, mean \pm SEM. One-way ANOVA was used for statistical analysis, and $p < 0.05$ was considered significant. (F) Immunofluorescence images (maximum intensity projections) showing stages of neuronal differentiation from neural stem cells. The cells were stained by the neuronal markers *TUBB3*/ β -tubulin III (green), *NEFH*/neurofilament heavy polypeptide (red) and *MAP2* (magenta) followed by counterstaining with DAPI (blue). The figures i to v represent 21 DIV, vi to x represent 30 DIV, xi to xv represent 45 DIV and xvi to xx represent 60 DIV. Scale bar: 20 μ m.

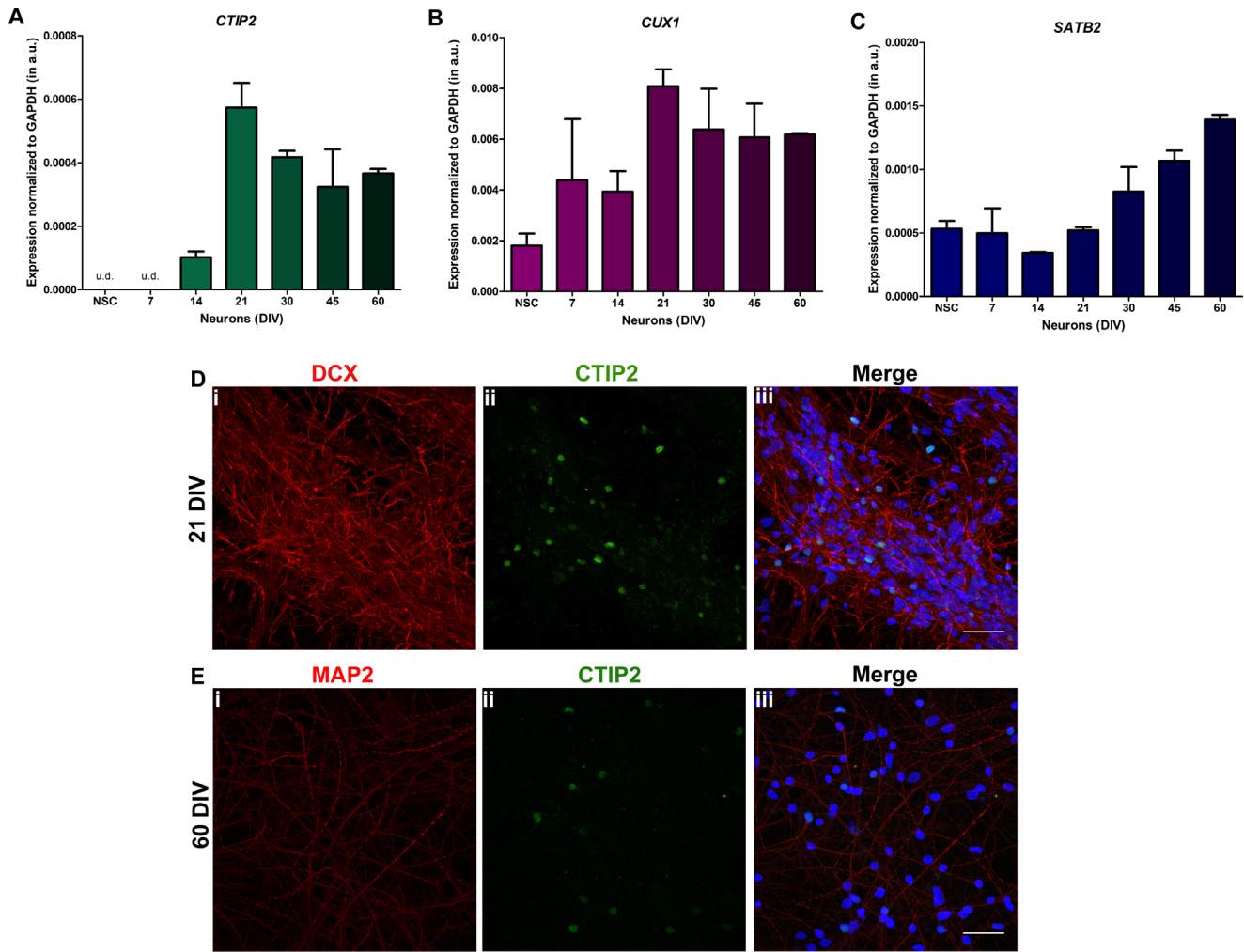


Figure 4. Expression of cortical layer neuronal markers (A) to (C) Relative mRNA expression levels of cortical neuronal layer markers *CTIP2*, *CUX1* and *SATB2* at various stages of neuronal differentiation obtained from quantitative real time PCR (qRT PCR). The expression levels have been normalized with *GAPDH* as endogenous control and the values represented in the terms of $2^{-\Delta C_t}$ -Y-axis, mean \pm SEM. One-way ANOVA was used for statistical analysis, and $p < 0.05$ was considered significant. **(D)** Representative images of immature neuronal marker DCX (red) and layer-V marker CTIP2 (green) observed in culture from 21 days *in vitro* (DIV) onwards. **(E)** 60 DIV neurons were immunostained with mature neuronal marker MAP2 (red) to validate presence of mature neurons expressing CTIP2 (green).

(SYP), and the post-synaptic density protein PSD-95. Levels of transcripts for these molecules were found to increase from about 21 DIV and peak between 45 to 60 DIV (Figure 5A–C). Immunofluorescence labelling also revealed the presence of punctate labelling for both SYN and SYP in 60 DIV neurons (Figure 5 D, E). The cerebral cortex consists of neurons that are both excitatory glutamatergic and inhibitory GABAergic (γ -aminobutyric-acid) with respect to neurotransmitter usage. In our *in vitro* cultures, we found that the expression of glutamate decarboxylase (*GAD67*), the enzyme that generates GABA from glutamate and glutaminase (*GLS*) that converts glutamine to glutamate, increase steadily from 14 DIV (Figure 5 F, G). Finally, expression of the transporter vGLUT1 that mediates the uptake of glutamate from the synaptic cleft steadily increased from 21 DIV (Figure 5 H).

We assessed the cellular composition of our *in vitro* differentiated cultures by quantifying the expression of markers for astrocytes (GFAP) and oligodendrocytes (OLIG2). The levels of GFAP transcripts were minimal prior to 21 DIV and then increased with the age of the culture (Figure 5I) while that for OLIG2 was minimal until 45 DIV (Figure 5J). GFAP staining was not detectable prior to 21 DIV, was minimal at 45 DIV and only increased from 60 DIV (Figure 5K i, v, ix). OLIG2 protein expression was not detectable even at 60 DIV (Figure 5K ii, vi, x).

Development of spontaneous neuronal activity *in vitro*

Spontaneous activity underpinned by changes in $[Ca^{2+}]_i$ play a critical role in synaptic development, remodelling²⁰ and neurotransmitter choice²¹ during neuronal development [reviewed in 22].

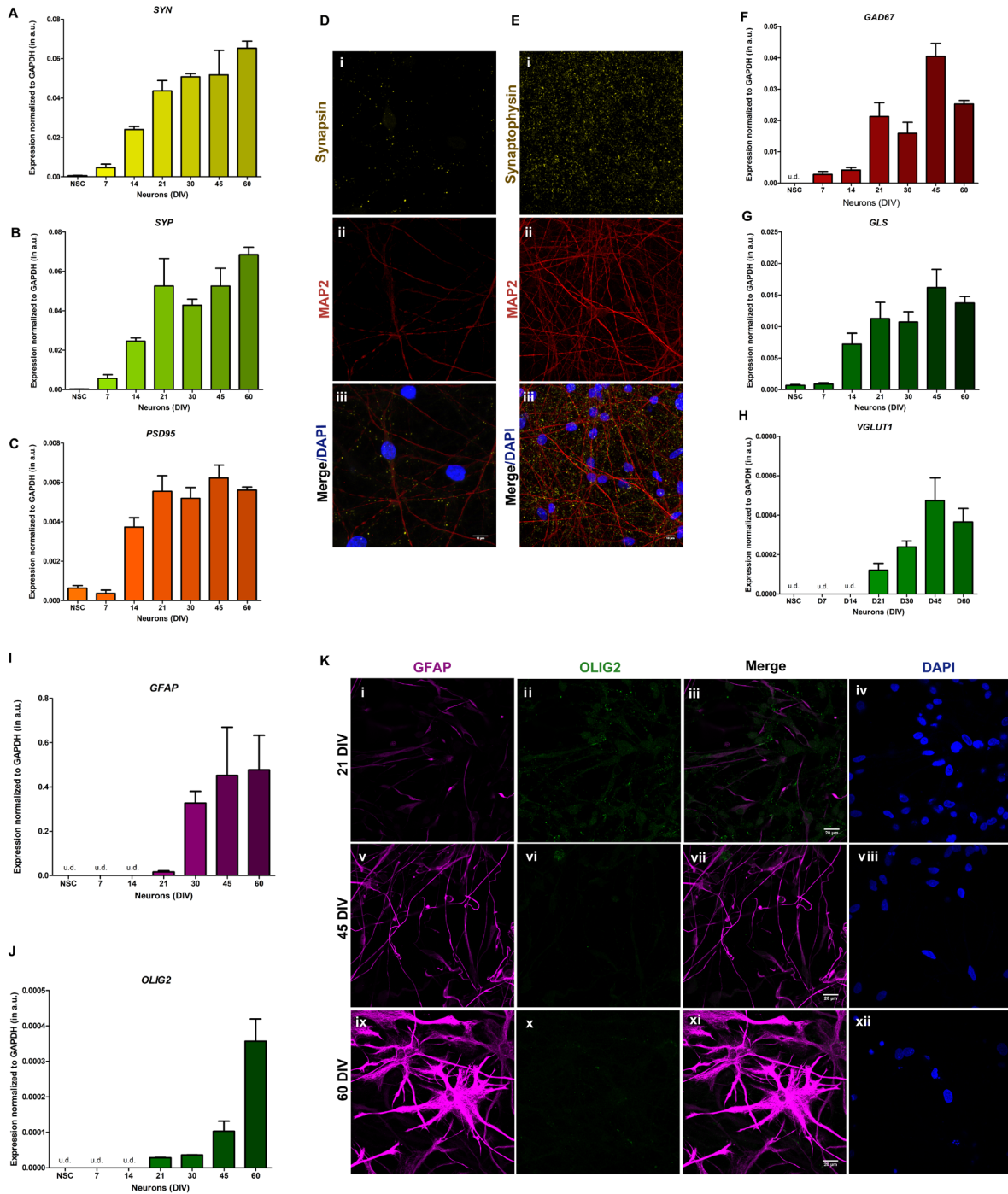


Figure 5. Expression of synaptic and glial markers during *in-vitro* differentiation. (A) to (C) Relative mRNA expression levels of synaptic markers *SYN*, *SYP* and *PSD95* at stages of neuronal differentiation obtained from quantitative real time PCR (qRT PCR). The expression levels have been normalized with *GAPDH* as endogenous control and the values represented in the terms of $2^{-\Delta\Delta C_T}$ -Y-axis, mean \pm SEM. (D) Presence of presynaptic protein Synapsin 1 (yellow) and (E) synaptic vesicle protein Synaptophysin (yellow) in MAP2 (red) positive neuronal cells. The nuclei of the cells were observed by staining with DAPI (blue). (F) to (H) qRT PCR results of relative mRNA expression in GABAergic neuronal marker *GAD67*, and glutamatergic neuronal markers *GLS* and *VGLUT1* respectively. (I) and (J) Relative mRNA expression levels of astrocyte and oligodendrocyte markers *GFAP* and *OLIG2* respectively at different stages of neuronal differentiation, as obtained from qRT PCR. The expression levels of all the genes have been normalized with *GAPDH* as endogenous control and the values represented in the terms of $2^{-\Delta\Delta C_T}$, mean \pm SEM. One-way ANOVA was used for statistical analysis, and $p < 0.05$ was considered significant. (K) Immunofluorescence images (maximum intensity projections) showing expression of GFAP (magenta) and OLIG2 (green) at stages of neuronal differentiation from neural stem cells. The cells were stained with astrocyte marker GFAP and oligodendrocyte marker OLIG2, followed by counterstaining with DAPI (blue). The figures i to iv represent to 21 DIV, v to viii represent 30 DIV, ix to xii represent 45 DIV and xiii to xvi represent 60 DIV. Scale bar: 20 μ m.

To measure spontaneous activity in our *in vitro* cultures, we measured fluctuations in $[Ca^{2+}]_i$. *In vitro* neuronal cultures at specified ages were loaded with fluorescent Ca^{2+} indicators and examined for evidence of spontaneous elevations of $[Ca^{2+}]_i$. Based on visual examination, two types of transients were noted: (i) those that were observed in neurites and (ii) those seen in the soma (Video 1, see extended data²³). In this study, we quantified $[Ca^{2+}]_i$ transients that arose in the soma. We found that in 7 DIV neurons a minimal number of such transients were seen (Figure 6A). The number of such transients progressively increased as a function of the age of the culture, i.e. older cultures showed more transients/unit time (Figure 6B-E, G). The resting membrane potentials (RMPs) of neurons during early stages of differentiation is reported to be depolarized and as neurons mature, their RMPs become hyperpolarized. This is validated by blocking the voltage-gated Na^+ channel using tetrodotoxin (TTX). In our cultures, we observe that the activity displayed in the baseline measurement was abolished by addition of TTX starting 14 DIV onwards specifically in neurons that fired trains of spontaneous transients, indicating a mixed culture with some neurons maturing faster than rest. TTX did not completely abolish these transients in the early days of neuronal differentiation. In contrast, TTX abolished the calcium oscillations virtually in all 30 DIV and 45 DIV neurons. (Figure 6A v 6D, E). A primary source of the spontaneous $[Ca^{2+}]_i$ seen in our cultures is likely to be the activity of voltage activated Ca^{2+} channels (VGCC). Consistent with this idea, we were able to abolish the $[Ca^{2+}]_i$ transients by the application of the VGCC blocker, nimodipine (Figure 6 F i, ii). Overall, we were able to maintain these cultures up to 120 DIV and observe $[Ca^{2+}]_i$ transients at each age of assessment. However, in older cultures, cellular crowding occurs and it became progressively more difficult to unambiguously assign ROI to a single soma using epifluorescence microscopy.

Store operated calcium influx in developing neurons

Many neuronal responses are modulated by the activation of cell surface receptors that couple to the G-protein subunit Gq, activating phospholipase C (PLC) and culminating in the influx of extracellular Ca^{2+} through a process of SOCE. To test the presence of SOCE in our *in vitro* cultures, we performed experiments where we depleted internal Ca^{2+} stores using the SERCA pump inhibitor thapsigargin and observed both intracellular release and the influx of Ca^{2+} into the cytosol from the extracellular space. In our experiments we observed that the average resting $[Ca^{2+}]_i$ was ca 26 nM; this rose to 48.5 nM in 14 DIV and was subsequently only slightly elevated thereafter up to 45 DIV (Figure 7B). In the initial part of the experiment, we applied thapsigargin to cultures loaded with Ca^{2+} indicator but bathed in zero extracellular Ca^{2+} . The rise in fluorescence represents the release of Ca^{2+} from intracellular stores and could be readily observed at all stages of differentiation (Figure 7A). We quantified this release which approximates the size of the ER Ca^{2+} pool and noted that the smallest elevation of $[Ca^{2+}]_i$ was seen in NSC and the largest in 45 DIV neurons (Figure 7D). Finally we measured the peak of the $[Ca^{2+}]_i$ following add back of extracellular Ca^{2+} and found that while minimal SOCE was seen in NSC, significant influx was only seen in 45 DIV (Figure 7A, C).

To understand the development of SOCE based Ca^{2+} influx, we measured the expression of the core elements of the SOCE pathway²⁴. SOCE is mediated by the ORAI channel. Three genes encode this protein in the human genome. Of these *ORAI1* and *ORAI3* were expressed in NSC with minimal expression of *ORAI2*. During differentiation *ORAI1* expression was enhanced at 45 DIV and while that of *ORAI3* at 30 DIV (Figure 7E). The activation of ORAI is mediated by store depletion, triggered *in vivo* by inositol 1,4,5 trisphosphate (IP_3) receptor mediated release of Ca^{2+} from internal stores. This store depletion is sensed by the ER localized Ca^{2+} sensor STIM which then leads to activation of ORAI. We measured the expression of IP_3 receptor and STIM in our cultures. While *ITPR1* and *ITPR3* were expressed at negligible levels, *ITPR2* expression increased steadily during differentiation (Figure 7F). Two genes encode for STIM in the human genome; of these *STIM1* which activates ORAI channels was expressed at very low levels in NSC and its expression increased steadily from 14 DIV onwards (Figure 7G). By contrast *STIM2* was expressed at low levels at all stages except at 30 DIV when its expression was substantially elevated (Figure 7G). Interestingly, at exactly that stage the level of *STIM1* dropped significantly (Figure 7G).

Molecular basis of spontaneous Ca^{2+} signals in developing neurons

A likely value of this experimental model is the ability to test for changes in Ca^{2+} signalling in human patients with specific diseases of the brain using patient derived iPSC differentiated into neurons. In addition to the activity of VGCC, $[Ca^{2+}]_i$ transients can also arise from the activity of N-methyl D-aspartate (NMDAR), Ca^{2+} permeable AMPAR, nAChR and the shape, size and frequency of the transients can be modulated by expression of other components of the Ca^{2+} signalling toolkit¹. Once changes in Ca^{2+} signalling are detected in neurons differentiated from patient cells, a natural next step is to probe the molecular basis of such changes. Towards this end, it is necessary to have a description of the Ca^{2+} signalling toolkit operating in neurons differentiated using this protocol so that observed changes may be mapped to specific molecular processes. To establish the likely molecular components that shape Ca^{2+} transients in the developing *in vitro* neuronal cultures, we performed an RNA-seq analysis of transcripts from NSC, 45 DIV and 60 DIV neurons.

We found ca. 6000 upregulated and ca. 3700 downregulated transcripts in 45 DIV (See underlying data) and 60 DIV neurons (See underlying data) compared to NSC. The vast majority of these altered transcripts were common to both 45 and 60 DIV neurons (Figure 8A, B) although a few were specifically changed in either 45 DIV or 60 DIV only. We curated a list of genes encoding molecules likely to directly regulate Ca^{2+} signalling. These are indicated in Figure 8C (upregulated genes) and Figure 8D (downregulated genes). We found that of the many possible genes in the human genome that could encode a specific component, transcripts for only a subset were expressed in 45 DIV or 60 DIV neurons; for example, of the 10 genes that encode different subunits of VGCC in the human genome, only six genes were expressed in differentiated neurons at 45 DIV and 60 DIV.

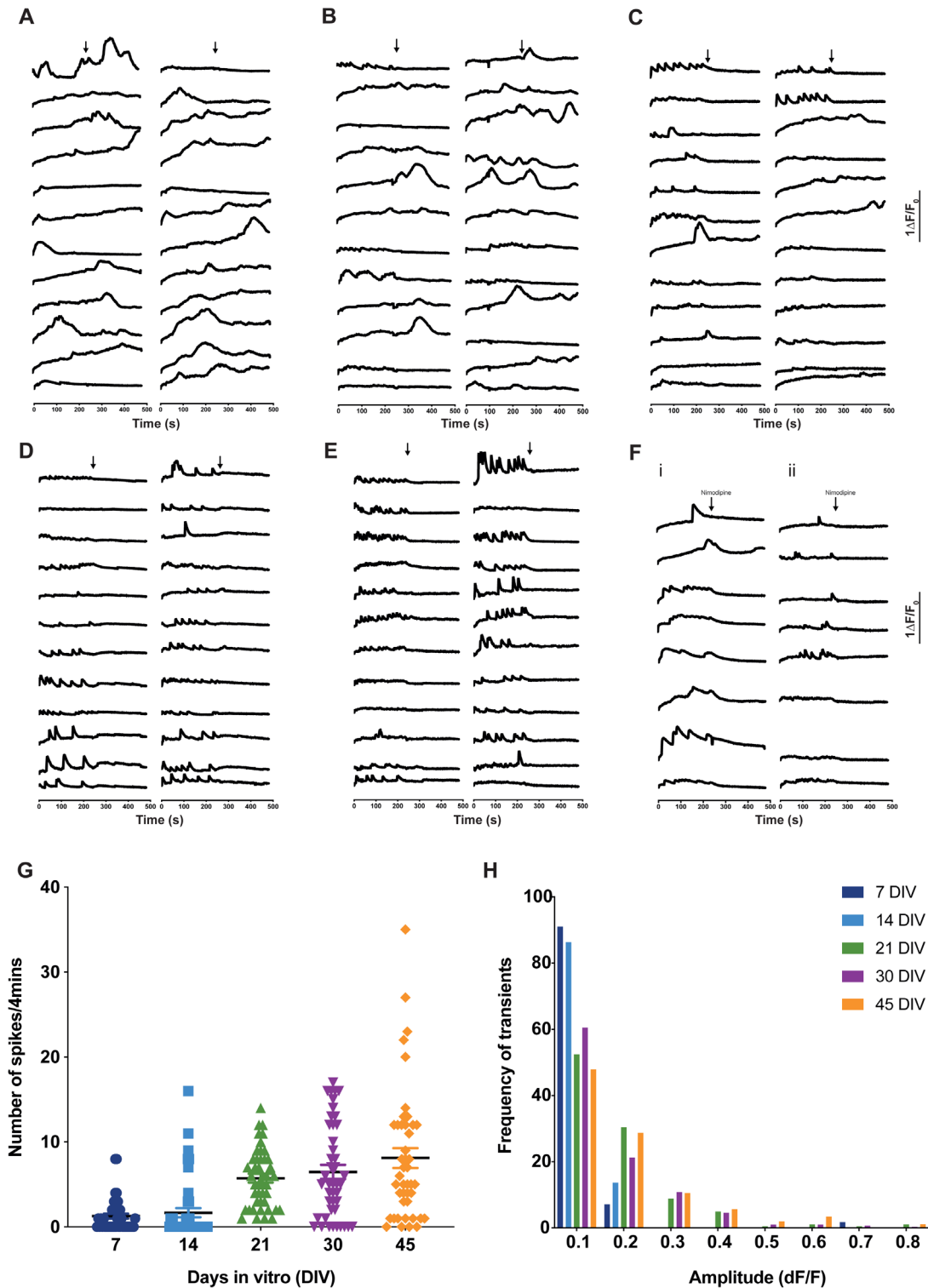


Figure 6. Development of Ca^{2+} transients during *in-vitro* differentiation. (A) to (E) Calcium transients recorded at 7, 14, 21, 30 and 45 DIV are shown. Each panel shows $[\text{Ca}^{2+}]_i$ traces from individual cells in the dish. Y-axis shows ΔF . X-axis is time in s. The baseline was recorded for 4 mins, followed by addition of $10\mu\text{M}$ tetrodotoxin (TTX) (as indicated by the arrows) to block Ca^{2+} transients. (F) Calcium transients recorded from 7 DIV (i) and 60 DIV (ii) cultures. Traces for individual cells are shown. An L-type VGCC blocker Nimodipine ($10\mu\text{M}$) was applied at the point indicated and completely abolished transients. (G) The number of spikes/ 4 min was counted from individual neurons at each age and plotted. Symbols on the scatter-dot plot correspond to individual neurons. Mean \pm SEM for 30–40 neurons. (H) Bar graph quantifying the amplitude of calcium transients that was analyzed and binned. X-axis shows the amplitude size of each bin. Y-axis shows the proportion of transients corresponding to that bin size at each age.

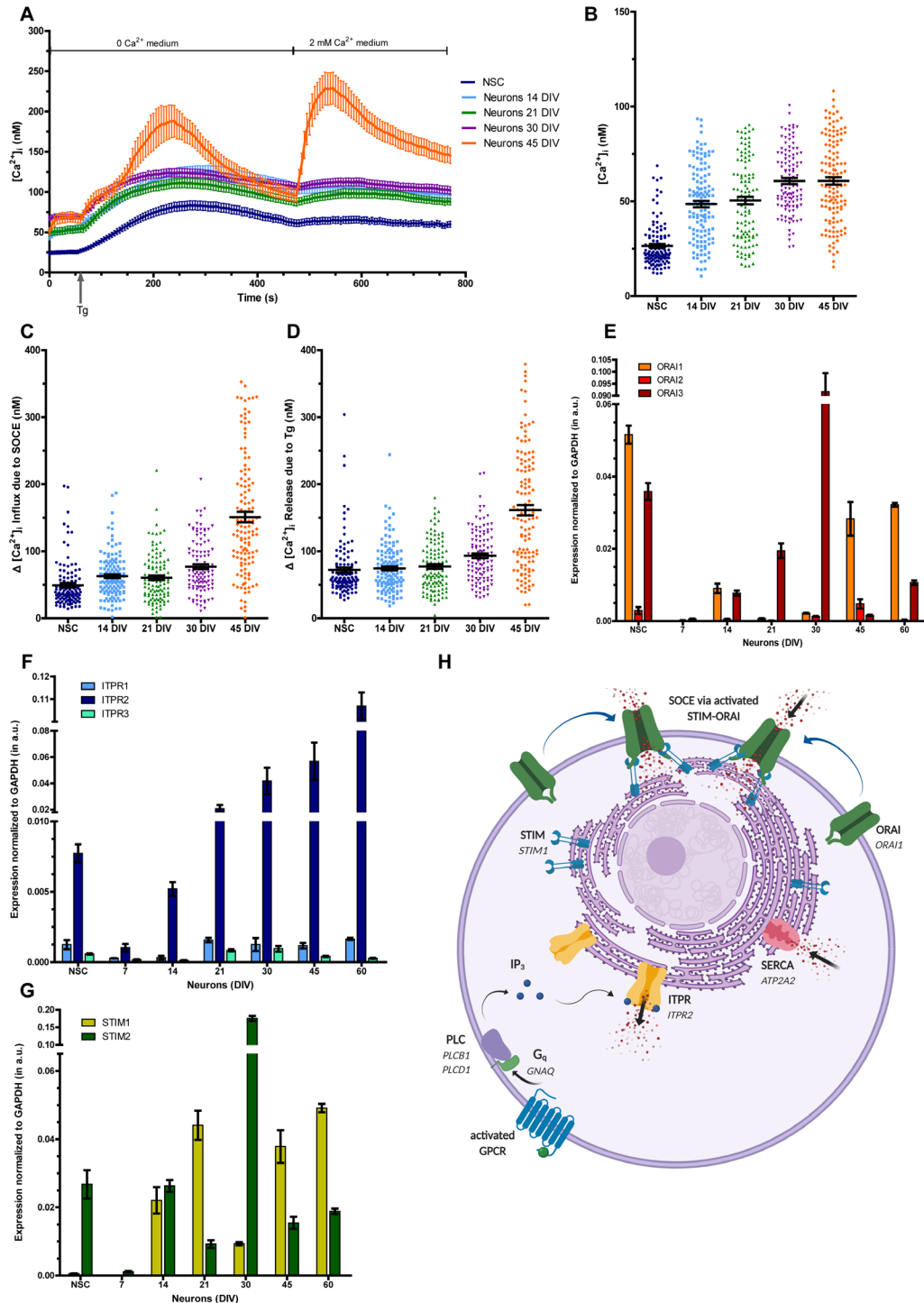


Figure 7. Characterization of store operated calcium entry (SOCE) in neural stem cells (NSCs) and *in vitro* differentiated cortical neurons. (A) $[Ca^{2+}]_i$ levels measured using the ratiometric dye Fura-2 during Thapsigargin induced store release and subsequent SOCE in XCL1 NSCs and *in vitro* differentiated cortical neurons of specific ages. Each trace for a given age consists of the mean \pm SEM for 25–30 cells. (B) Scatter plot quantifying the resting cytosolic $[Ca^{2+}]_i$; each point represents a single cell in the culture. X-axis shows age of neurons in culture (DIV). (C,D) Scatter plots quantifying $[Ca^{2+}]_i$ rise above basal cytosolic $[Ca^{2+}]_i$ for (C) SOCE and (D) Tg mediated store release respectively at various ages of *in vitro* culture. qPCR measurements to show the relative expression of various isoforms of Orai (E), STIM (G) and the IP₃ receptor (ITPR) (F) at different stages of differentiation. (H) Cartoon (created using Biorender) representing the components of SOCE that are expressed in differentiating NSC. Individual organelles and membranes are shown. The individual component of SOCE are shown in capital, bold. The genes predominantly encoding each component in these cells are shown in *italics*. (Abbreviations: G_q is G protein α -subunit, encoded by the gene GNAQ; PLC is Phospholipase C, the predominantly expressed isoforms are PLC β ₁ and PLC δ ₁, encoded respectively by PLCB1 and PLCD1; SERCA (Sarco/Endoplasmic Reticulum Ca²⁺-ATPase) is encoded mainly by the gene ATP2A2.)

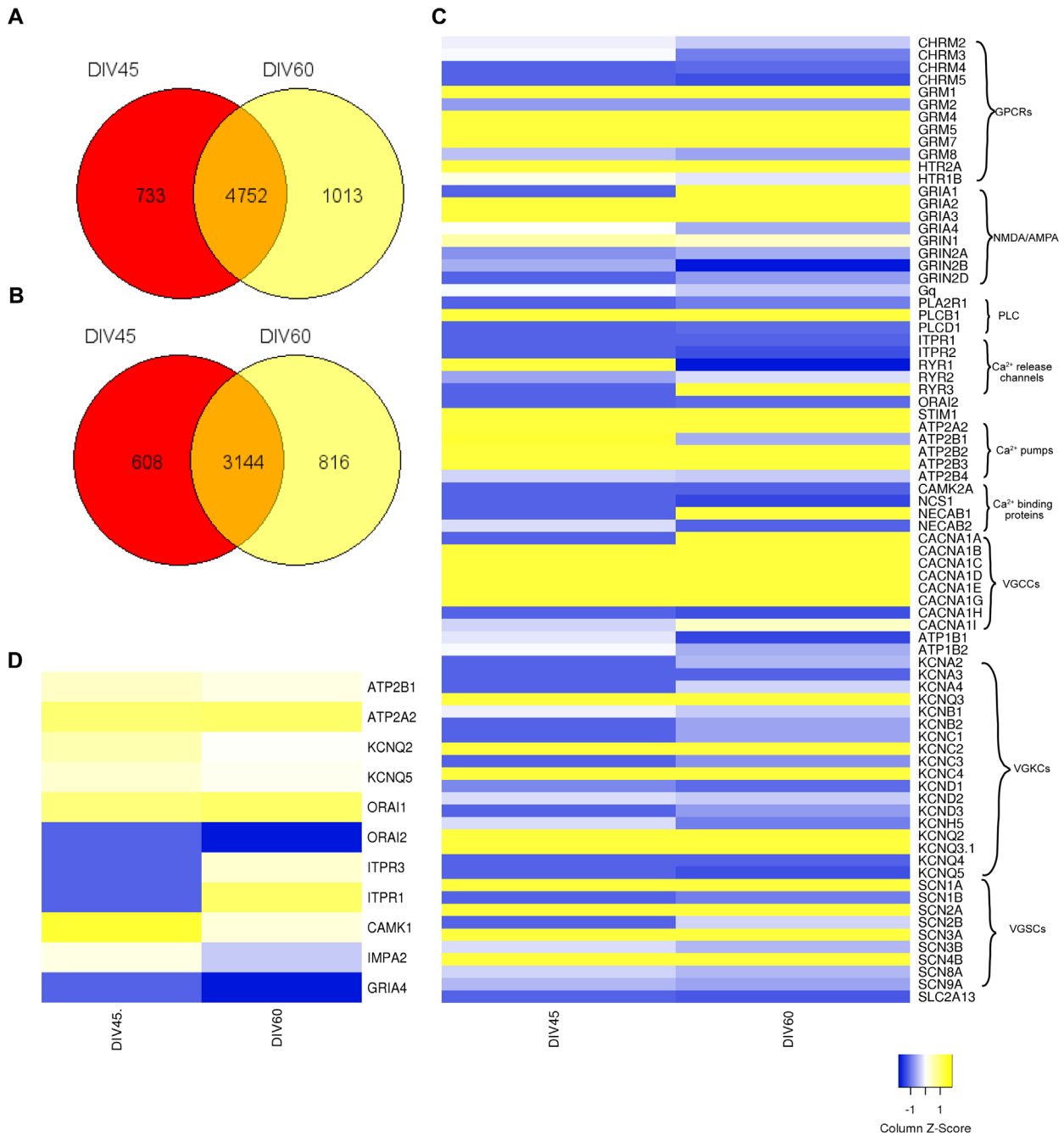


Figure 8. Heatmap to showing the calcium signalling transcriptome of neural stem cells (NSCs) and neurons at 45 days *in vitro* (DIV) and 60 DIV. **(A)** Venn diagram to show the number of common upregulated genes between sample 45 DIV and 60 DIV: The total number of upregulated genes ($\log_2 FC > +1.5$) were counted in each sample and the number of common upregulated genes were calculated between 45 DIV and 60 DIV. These values have been plotted as Venn diagram. **(B)** Venn diagram to show number of common downregulated genes between sample 45 DIV and 60 DIV: The total number of downregulated genes ($\log_2 FC < -1.5$) were counted in each sample and the number of common downregulated genes were calculated between 45 DIV45 and 60 DIV. These values have been plotted as Venn diagram. **(C)** Upregulated genes: The heatmap represents the extent of upregulation of genes directly involved in calcium signalling in 45 DIV and 60 DIV samples compared to NSCs. The values have been scaled by column Z-score and scale ranges from -1 to +1 (blue to yellow). The gene names as from HUGO nomenclature are represented on Y-axis. The heatmap was made using heatmapR. The genes have been grouped into the following categories: GPCRs (G-Protein Coupled Receptors), AMPA/NMDA receptors, PLC (Phospholipases), Ca^{2+} release channels, Ca^{2+} pumps, Ca^{2+} binding proteins, VGCCs (Voltage-Gated Calcium Channels), VGKCs (Voltage-Gated Potassium Channels) and VGSCs (Voltage-Gated Sodium Channels). **(D)** Downregulated genes: The heatmap represents the extent of downregulation of genes involved in calcium signalling in 45 DIV and 60 DIV samples compared to NSCs. The values have been scaled by column Z-score and scale ranges from -1 to +1 (blue to yellow). The gene names as from ensemble nomenclature are represented on Y-axis. The heatmap was made using heatmapR.

Two of them were expressed only in 60 DIV and one of them was highly upregulated in 60 DIV as compared to 45 DIV (Figure 8C). Thus, analysis of VGCC activity and its role in mediating any Ca^{2+} signalling phenotype can now be focused to these genes, for example by RNAi mediated depletion or CRISPR/Cas9 gene editing.

Discussion

Brain structure and function can be investigated at multiple scales of analysis including behavioural output, structural and functional imaging (e.g MRI) and clinical electrophysiology and these have been extensively used in the analysis of brain disease biology. However, a long-standing challenge in studying human brain disease is the ability to study mechanisms at the level of cellular and molecular processes in living human brain cells that typically require neural cells in a dish. The advent of modern stem cell technology that allows the generation of iPSC from the somatic cells of humans and their subsequent differentiation into neural cell types *in vitro* offers a solution to this problem⁸. The human brain consists of multiple cell types including neurons, glial cells and vasculature. In additions, for a single cell type such as neurons, each region of the brain contains neurons of distinct molecular identities and physiological properties. To facilitate this, we have developed a protocol that allows human cortical neurons to be differentiated starting with NSC, a stem cell population observed during brain development²⁵. Our protocol described here allows developing neurons to be maintained in culture for almost 120 DIV. This corresponds to 15–16 post-conception weeks of the human brain development²⁶. These cultures can be studied using live imaging methods to observe and quantify cell biological and physiological processes upto this age *in vitro* and thus allow the reconstruction of physiological development of these neurons. This strategy will allow the comparison of neuronal development between NSC derived from normal human subjects as well as those derived from patients with specific brain disorders. Given the proposed developmental origins of many human brain diseases²⁷, our approach will allow the analysis of defects in cell physiology in developing neurons.

The human cerebral cortex is a complex cellular structure composed of six layers each of which contains specialized neuronal types with distinct functional properties and projections. In using *in vitro* cultures to study the properties of human brain cells differentiated from NSCs, it is necessary to establish the extent to which these cultures differentiate to form the cell types typical of the human cerebral cortex. The cell types of the cerebral cortex are specified by transcription factors that are typical for particular cell types or layers. Using qRT-PCR and immunocytochemistry, we found that our cultures show progressively increasing expression of Cut like homeobox 1 (CUX) [required for dendritic morphogenesis in layer II-III cortical neurons], CTIP2 a transcription factor typical of layers V-VI and *SATB2* of cortical layer II-IV. These findings suggest that our protocol generates *in vitro* cultures with cell types representative of several key layers of the human cerebral cortex. Thus, the physiological properties of the neurons generated by this method are likely to reflect at least some of the properties of neurons in the human cerebral cortex. In this respect, these culture will likely be useful for the analysis of physiological changes in human brain

disorders where the cerebral cortex is primarily affected. These include several key examples of severe mental illness including schizophrenia, bipolar disorder, neurodevelopmental disorders that affect cortical development and function as well as neurological disorders such as epilepsy.

In this study, we have imaged and quantified the frequency and amplitude of $[\text{Ca}^{2+}]_i$ transient development. We found that in our culture conditions, the frequency of $[\text{Ca}^{2+}]_i$ transients increased as a function of the age of the culture (DIV) (Figure 6 G,H). The $[\text{Ca}^{2+}]_i$ transients were blocked by the addition of nimodipine, a blocker of VGCC suggesting that the activity of VGCC underlies their generation. In addition, the $[\text{Ca}^{2+}]_i$ were also abolished by the application of TTX, a blocker of Na^+ channels suggesting that voltage changes presumably through the depolarization of neurons likely activates VGCC resulting in the $[\text{Ca}^{2+}]_i$ observed by imaging. Overall these findings imply the progressive development of neuronal activity in the *in vitro* cultures as a function of age that can be monitored using Ca^{2+} imaging. Thus our culture system and the use of $[\text{Ca}^{2+}]_i$ transient imaging is likely to be of value in observing altered development of neuronal activity in cell lines derived from patients with specific brain disorders. In addition, through DNA sequencing, a number of mutations have been described in genes encoding components of the Ca^{2+} signalling machinery in human patients. For example, numerous mutations have been described in *CACNA1B* (calcium channel, voltage-dependent, N-type, alpha 1B subunit) among patients with bipolar disorder, autism spectrum and Timothy syndrome⁷. Interestingly, a recent study has described a role for VGCC in the development of mouse cortical neurons through the control of cellular processes such as neurite outgrowth and radial migration²⁸. The methods described in this paper will allow the impact of human mutations in calcium signalling genes (such as *CACNA1B*) to be studied in the context of neuronal development and physiology.

In addition to VGCC, many other mechanisms mediate changes in $[\text{Ca}^{2+}]_i$. SOCE is one of these processes and is triggered by G-protein coupled PLC activation, a signalling mechanism used by several cell surface receptors that are expressed in the human cerebral cortex and reported to be important for brain function [e.g metabotropic glutamate receptor] and PLC signalling has also been linked to several brain disorders²⁹. Studies in murine neural precursor cells (NPCs) have shown robust SOCE and depletion of *STIM1* or *ORAI1*, key elements of SOCE results in defective NPC proliferation³⁰; a recent study has also suggested a conserved role for SOCE in human NPC proliferation³¹. In this study we developed protocols to monitor SOCE during *in vitro* differentiation and found a dynamic pattern of SOCE activity. Thus, our culture system and imaging protocols can be used to study the role of SOCE in cells derived from patients with specific human brain diseases. In addition, PLC signalling also triggers phosphoinositide turnover and the mechanism of action of lithium, used in the management of bipolar disorder, is thought to occur via the modulation of inositol recycling in this setting [reviewed in 32]. This question can therefore be analysed using the protocols described here coupled with the analysis of phosphoinositide turnover using biochemical approaches.

Human brain diseases may arise from multiple mechanisms including both cell-autonomous processes in neurons and also as an outcome of neuronal dysfunction arising through cell-cell interaction mechanisms between neurons and other cell types. Regardless of these different mechanisms, studying any given cell-biological process in human neurons requires the generation of *in vitro* neuronal live cultures in which physiological processes can be studied in the context of neuronal development. In our protocol, we found that there was minimal presence of non-neuronal cells until ca. 21 DIV but from 30 DIV transcripts for GFAP increased and GFAP immunoreactivity was seen from 45 DIV onwards. This time course of gliogenesis observed in our culture system is consistent with previous studies that have reported a substantial increase in GFAP+ cells over time following the initial appearance of neuronal cells during brain development both *in vivo*³³ and *in vitro*³⁴. Thus upto ca. 30 DIV our cultures will be suitable for the analysis of cell-autonomous phenotypes arising from neurons but thereafter, phenotypes observed may reflect contributions from both neurons and glial cells present in the cultures. Interestingly, an increasing number of brain diseases are linked to neuron-glia interactions^{35,36} and could be studied in older cultures of the type we observed post 30 DIV.

In summary, we have developed a protocol that allows the quantitative analysis of Ca²⁺ signalling defects in neural cells in the context of human diseases that affect the brain. The use of this approach should provide mechanistic insights into the cell biology and physiology of human neurodevelopmental disorders and may further lead to the development of therapeutic approaches for these conditions.

Data availability

Underlying data

Open Science Framework: Calcium imaging data_Sharma et.al.2019_NCBS TIFR. <https://doi.org/10.17605/OSF.IO/V7XE6>²³

This project contains the following underlying data:

- Figure panel 1
 - Cell proliferation data.xlsx (growth curve of XCL1 NSCs)
 - [Figure 1C](#) (Folder containing Immunofluorescence confocal images for characterization of neural stem cell markers)
 - Karyotype report.pdf (cytogenetic characterization of XCL1 NSCs)
- Figure panel 3 (Folder containing immunofluorescence confocal images of neuronal markers)

- Figure panel 4 (Folder containing Immunofluorescence confocal images of cortical layer marker)
- Figure panel 5 (Folder containing the confocal images listed below)
 - [Figure 5D,E](#) (Immunofluorescence confocal images of synaptic markers)
 - [Figure 5K](#) (Immunofluorescence confocal images of glial markers)
 - Figure panel 6 (Folder containing Excel files for Ca²⁺ imaging for Ca²⁺ transient activity)
- Figure panel 7 (Folder containing Excel files for SOCE characterization)
- qRT-PCR data
 - Ct values for qRT-PCR experiments.xlsx (Excel file containing raw Ct values for qRT-PCR)
 - ITPR neurons expression qpcr raw ct values.xlsx (Excel file containing raw Ct values for qRT-PCR measuring ITPR expression)
 - STIM and ORAI expression qpcr raw ct values.xlsx (Excel file containing raw Ct values for qRT-PCR measuring STIM and ORAI expression)

Extended data

Open Science Framework: Calcium imaging data_Sharma et al. 2019_NCBS TIFR. <https://doi.org/10.17605/OSF.IO/V7XE6>²³

This project contains the following extended data:

- Sharma_Video1.avi (Calcium imaging recordings of 45 DIV cortical neurons showing spontaneous activities in the soma as well as the neurites. Cells were loaded with Fluo-4/AM and imaged at 1 fps for 480 s)

Data are available under the terms of the [Creative Commons Zero “No rights reserved” data waiver](#) (CC0 1.0 Public domain dedication).

RNA sequencing data has been submitted to the Sequence Read Archive database on NCBI under project ID [PRJNA600215](#).

RNA-seq of neurons, Accession number SRX7527467: <https://identifiers.org/insdc.sra:SRX7527467>

RNA-seq of XCL1, Accession number SRX7527466: <https://identifiers.org/insdc.sra:SRX7527466>

References

1. Bootman MD, Bultynck G: **Fundamentals of Cellular Calcium Signaling: A Primer.** *Cold Spring Harb Perspect Biol.* 2020 [cited 2019 Nov 7]; **12**(1): pii: a038802. [PubMed Abstract](#) | [Publisher Full Text](#)
2. Berridge MJ, Bootman MD, Lipp P: **Calcium—a life and death signal.** *Nature.* 1998; **395**(6703): 645–8. [PubMed Abstract](#) | [Publisher Full Text](#)
3. Alves VS, Alves-Silva HS, Orts DJB, et al.: **Calcium Signaling in Neurons and**

- Glial Cells: Role of Cav1 channels.** *Neuroscience*. 2019 [cited 2019 Nov 9]; 421: 95–111.
[PubMed Abstract](#) | [Publisher Full Text](#)
4. Pchitskaya E, Popugaeva E, Bezprozvanny I: **Calcium signaling and molecular mechanisms underlying neurodegenerative diseases.** *Cell Calcium*. 2018 [cited 2019 Nov 9]; 70: 87–94.
[PubMed Abstract](#) | [Publisher Full Text](#) | [Free Full Text](#)
 5. Berridge MJ: **Calcium signalling and psychiatric disease: bipolar disorder and schizophrenia.** *Cell Tissue Res*. 2014 [cited 2019 Nov 9]; 357(2): 477–92.
[PubMed Abstract](#) | [Publisher Full Text](#)
 6. Steinlein OK: **Calcium signaling and epilepsy.** *Cell Tissue Res*. 2014 [cited 2019 Nov 9]; 357(2): 385–93.
[PubMed Abstract](#) | [Publisher Full Text](#)
 7. Hörtenhuber M, Toledo EM, Smedler E, *et al.*: **Mapping genes for calcium signaling and their associated human genetic disorders.** Hancock J, editor. *Bioinformatics*. 2017 [cited 2019 Nov 9]; 33(16): 2547–54.
[PubMed Abstract](#) | [Publisher Full Text](#) | [Free Full Text](#)
 8. Russo FB, Cugola FR, Fernandes IR, *et al.*: **Induced pluripotent stem cells for modeling neurological disorders.** *World J Transplant*. 2015; 5(4): 209–21.
[PubMed Abstract](#) | [Publisher Full Text](#) | [Free Full Text](#)
 9. Grynkiewicz G, Poenie M, Tsien RY: **A new generation of Ca²⁺ indicators with greatly improved fluorescence properties.** *J Biol Chem*. 1985 [cited 2019 Nov 16]; 260(6): 3440–50.
[PubMed Abstract](#)
 10. Wingett SW, Andrews S: **FastQ Screen: A tool for multi-genome mapping and quality control [version 1; peer review: 3 approved, 1 approved with reservations].** *F1000Res*. 2018 [cited 2019 Nov 16]; 7: 1338.
[PubMed Abstract](#) | [Publisher Full Text](#) | [Free Full Text](#)
 11. Li B, Dewey CN: **RSEM: accurate transcript quantification from RNA-Seq data with or without a reference genome.** *BMC Bioinformatics*. 2011 [cited 2019 Nov 16]; 12(1): 323.
[PubMed Abstract](#) | [Publisher Full Text](#) | [Free Full Text](#)
 12. Anders S, Huber W: **Differential expression analysis for sequence count data.** *Genome Biol*. 2010 [cited 2019 Nov 16]; 11(10): R106.
[PubMed Abstract](#) | [Publisher Full Text](#) | [Free Full Text](#)
 13. Berridge MJ, Lipp P, Bootman MD: **The versatility and universality of calcium signalling.** *Nat Rev Mol Cell Biol*. 2000 [cited 2019 Nov 16]; 1(1): 11–21.
[PubMed Abstract](#) | [Publisher Full Text](#)
 14. des Portes V, Pinard JM, Billuart P, *et al.*: **A novel CNS gene required for neuronal migration and involved in X-linked subcortical laminar heterotopia and lissencephaly syndrome.** *Cell*. 1998 [cited 2019 Aug 4]; 92(1): 51–61.
[PubMed Abstract](#) | [Publisher Full Text](#)
 15. Gleeson JG, Allen KM, Fox JW, *et al.*: **Doublecortin, a brain-specific gene mutated in human X-linked lissencephaly and double cortex syndrome, encodes a putative signaling protein.** *Cell*. 1998 [cited 2019 Aug 4]; 92(1): 63–72.
[PubMed Abstract](#) | [Publisher Full Text](#)
 16. Duan W, Zhang YP, Hou Z, *et al.*: **Novel Insights into NeuN: from Neuronal Marker to Splicing Regulator.** *Mol Neurobiol*. 2016; cited 2019 Aug 4; 53(3): 1637–47.
[PubMed Abstract](#) | [Publisher Full Text](#)
 17. Cubelos B, Sebastián-Serrano A, Beccari L, *et al.*: **Cux1 and Cux2 regulate dendritic branching, spine morphology, and synapses of the upper layer neurons of the cortex.** *Neuron*. 2010 [cited 2019 Aug 4]; 66(4): 523–35.
[PubMed Abstract](#) | [Publisher Full Text](#) | [Free Full Text](#)
 18. Alcamo EA, Chirivella L, Dautzenberg M, *et al.*: **Satb2 regulates callosal projection neuron identity in the developing cerebral cortex.** *Neuron*. 2008 [cited 2019 Nov 3]; 57(3): 364–77.
[PubMed Abstract](#) | [Publisher Full Text](#)
 19. Britanova O, de Juan Romero C, Cheung A, *et al.*: **Satb2 is a postmitotic determinant for upper-layer neuron specification in the neocortex.** *Neuron*. 2008 [cited 2019 Nov 3]; 57(3): 378–92.
[PubMed Abstract](#) | [Publisher Full Text](#)
 20. Gomez TM, Spitzer NC: **In vivo regulation of axon extension and pathfinding by growth-cone calcium transients.** *Nature*. 1999; 397(6717): 350–5.
[PubMed Abstract](#) | [Publisher Full Text](#)
 21. Gu X, Spitzer NC: **Distinct aspects of neuronal differentiation encoded by frequency of spontaneous Ca²⁺ transients.** *Nature*. 1995 [cited 2019 Nov 7]; 375(6534): 784–7.
[PubMed Abstract](#) | [Publisher Full Text](#)
 22. Rosenberg SS, Spitzer NC: **Calcium signaling in neuronal development.** *Cold Spring Harb Perspect Biol*. 2011 [cited 2019 Nov 7]; 3(10): a004259.
[PubMed Abstract](#) | [Publisher Full Text](#) | [Free Full Text](#)
 23. Sharma Y, Sankhanil S, Joseph A, *et al.*: **Calcium imaging & RNA-seq data_ Sharma et.al.2019_NCBS TIFR**. 2020.
<http://www.doi.org/10.17605/OSF.IO/V7XE6>
 24. Hogan PG, Rao A: **Store-operated calcium entry: Mechanisms and modulation.** *Biochem Biophys Res Commun*. 2015 [cited 2019 Nov 7]; 460(1): 40–9.
[PubMed Abstract](#) | [Publisher Full Text](#) | [Free Full Text](#)
 25. Tao Y, Zhang SC: **Neural Subtype Specification from Human Pluripotent Stem Cells.** *Cell Stem Cell*. 2016 [cited 2019 Nov 30]; 19(5): 573–86.
[PubMed Abstract](#) | [Publisher Full Text](#) | [Free Full Text](#)
 26. Silbereis JC, Pochareddy S, Zhu Y, *et al.*: **The Cellular and Molecular Landscapes of the Developing Human Central Nervous System.** *Neuron*. 2016 [cited 2019 Nov 23]; 89(2): 248–68.
[PubMed Abstract](#) | [Publisher Full Text](#) | [Free Full Text](#)
 27. Cicchetti D, Cannon TD: **Neurodevelopmental processes in the ontogenesis and epigenesis of psychopathology.** *Dev Psychopathol*. 1999 [cited 2014 Sep 15]; 11(3): 375–93.
[PubMed Abstract](#) | [Publisher Full Text](#)
 28. Kamijo S, Ishii Y, Horigane S, *et al.*: **A Critical Neurodevelopmental Role for L-Type Voltage-Gated Calcium Channels in Neurite Extension and Radial Migration.** *J Neurosci*. 2018 [cited 2019 Nov 15]; 38(24): 5551–66.
[PubMed Abstract](#) | [Publisher Full Text](#)
 29. Yang YR, Kang DS, Lee C, *et al.*: **Primary phospholipase C and brain disorders.** *Adv Biol Regul*. 2016 [cited 2019 Nov 16]; 61: 80–5.
[PubMed Abstract](#) | [Publisher Full Text](#)
 30. Somasundaram A, Shum AK, McBride HJ, *et al.*: **Store-operated CRAC channels regulate gene expression and proliferation in neural progenitor cells.** *J Neurosci*. 2014 [cited 2019 Nov 16]; 34(27): 9107–23.
[PubMed Abstract](#) | [Publisher Full Text](#) | [Free Full Text](#)
 31. Gopurappilly R, Deb BK, Chakraborty P, *et al.*: **Stable STIM1 Knockdown in Self-Renewing Human Neural Precursors Promotes Premature Neural Differentiation.** *Front Mol Neurosci*. 2018 [cited 2019 Nov 16]; 11: 178.
[PubMed Abstract](#) | [Publisher Full Text](#) | [Free Full Text](#)
 32. Raghu P, Joseph A, Krishnan H, *et al.*: **Phosphoinositides: Regulators of Nervous System Function in Health and Disease.** *Front Mol Neurosci*. 2019 [cited 2019 Nov 16]; 12: 208.
[PubMed Abstract](#) | [Publisher Full Text](#) | [Free Full Text](#)
 33. Honig LS, Herrmann K, Shatz CJ: **Developmental changes revealed by immunohistochemical markers in human cerebral cortex.** *Cereb Cortex*. 1996 [cited 2019 Nov 16]; 6(6): 794–806.
[PubMed Abstract](#) | [Publisher Full Text](#)
 34. Paşca AM, Sloan SA, Clarke LE, *et al.*: **Functional cortical neurons and astrocytes from human pluripotent stem cells in 3D culture.** *Nat Methods*. 2015 [cited 2019 Nov 16]; 12(7): 671–8.
[PubMed Abstract](#) | [Publisher Full Text](#) | [Free Full Text](#)
 35. Patel DC, Tewari BP, Chaunsali L, *et al.*: **Neuron-glia interactions in the pathophysiology of epilepsy.** *Nat Rev Neurosci*. 2019 [cited 2019 Nov 16]; 20(5): 282–97.
[PubMed Abstract](#) | [Publisher Full Text](#)
 36. Ioannou MS, Jackson J, Sheu SH, *et al.*: **Neuron-Astrocyte Metabolic Coupling Protects against Activity-Induced Fatty Acid Toxicity.** *Cell*. 2019 [cited 2019 Nov 16]; 177(6): 1522–1535.e14.
[PubMed Abstract](#) | [Publisher Full Text](#)

Open Peer Review

Current Peer Review Status:   

Version 1

Reviewer Report 23 March 2020

<https://doi.org/10.21956/wellcomeopenres.17119.r37771>

© 2020 Prakriya M. This is an open access peer review report distributed under the terms of the [Creative Commons Attribution License](#), which permits unrestricted use, distribution, and reproduction in any medium, provided the original work is properly cited.



Murali Prakriya

Department of Pharmacology, Feinberg School of Medicine, Northwestern University, Chicago, IL, USA

This is a nice review of procedures for differentiating neural progenitor lines into neurons and a careful description of the molecular and physiological properties of the differentiated neurons as they go through the differentiation process. It is well-written, very detailed, and will be useful for several investigators interested in the field as well as also providing a general list of tools, reagents, and procedures that could be applied more generally to workers in other related areas. I only have a few minor comments and suggestions.

1. Page 9. In the Grynkiewicz equation, the term ca^{2+} , the "C" should be capitalized.
2. Related, it is curious that the authors chose to use a K_d of 225 nM. Many other labs use an in vitro value of 135 nM. Please provide a citation for the use of 225 nM.
3. In Figure 6A-F, it is relatively hard to see how the arrow (indicating time of application) of TTX corresponds to the traces at the bottom of each panel. A dotted line going through all the traces in each panel would provide better clarity.
4. Likewise, in Figure 7A, please show the application of thapsigargin at the top, along the bars showing 0 mM Ca^{2+} /2 mM Ca etc. It is hard to see the arrow at the bottom axis.
5. Page 19, second paragraph on the left, 2nd line. *spealized* → *spealized*. Typo.

Is the rationale for developing the new method (or application) clearly explained?

Yes

Is the description of the method technically sound?

Yes

Are sufficient details provided to allow replication of the method development and its use by others?

Yes

If any results are presented, are all the source data underlying the results available to ensure full reproducibility?

Yes

Are the conclusions about the method and its performance adequately supported by the findings presented in the article?

Yes

Competing Interests: No competing interests were disclosed.

Reviewer Expertise: Neurophysiology, calcium signaling

I confirm that I have read this submission and believe that I have an appropriate level of expertise to confirm that it is of an acceptable scientific standard.

Reviewer Report 13 March 2020

<https://doi.org/10.21956/wellcomeopenres.17119.r38053>

© 2020 Borodinsky L. This is an open access peer review report distributed under the terms of the [Creative Commons Attribution License](#), which permits unrestricted use, distribution, and reproduction in any medium, provided the original work is properly cited.



Laura N. Borodinsky

Department of Physiology and Membrane Biology, Institute for Pediatric Regenerative Medicine, Shriners Hospital for Children, School of Medicine, University of California, Davis, Sacramento, CA, USA

The manuscript by Sharma *et al.* “**In vitro human stem cell derived cultures to monitor calcium signaling in neuronal development and function**” provides a methodological resource to assess calcium dynamics in human iPSC-derived cultured neurons. This approach might enable the modelling of human neurological diseases, specifically neurodevelopmental disorders, given that these cultures can be maintain for up to 120 days, which corresponds to 15-16 weeks of gestation.

This is a useful resource that may be of interest to diverse fields including, developmental biology and neuroscience, stem cell research and neurophysiology.

There are some specific issues that should be addressed:

1. In Methods, section “*E) Calculation of cell proliferation rate*”, “the authors proposed to count cells to determine proliferation rate. This is inadequate, number of cells can change by differences in proliferation rate and differences in cell survival. The authors will not be able to distinguish between these two cellular events from counting cells. More specialized approaches are required to sort these two cellular processes out.

2. GFAP and OLIG2 are not exclusive markers for astrocytes and oligodendrocytes, respectively. The authors should acknowledge the limitations of using these markers for identifying these cell types.
3. Page 13, 1st column, last sentence should be revised: “*Finally, expression of the transporter vGLUT1 that mediates the uptake of glutamate from the synaptic cleft steadily increased from 21 DIV (Figure 5 H)*”. This is wrong, VGLUT1 uptakes glutamate into vesicles inside the presynaptic glutamatergic neuron to enable release upon stimulation.
4. Figure 6H should be removed. A non-ratiometric dye like Fluo4-AM does not really allow for analysis of calcium transient amplitudes in different samples/culture dishes because of the variability in the loading of the dye in different cultures. The differences observed might not reflect the actual magnitude of changes in $[Ca^{2+}]_i$, but instead represent a technical difference in the loading of the dye in different cultures of different age, etc.
5. Figure 8C,D. Why are there some genes (ORAI2, ITRP1) in both C and D if one shows the upregulated (C) and the other the downregulated genes (D)?
6. “*Thus upto ca. 30 DIV our cultures will be suitable for the analysis of cell-autonomous phenotypes arising from neurons but thereafter, phenotypes observed may reflect contributions from both neurons and glial cells present in the cultures*”. The authors should revise the “cell-autonomous” term by replacing it with neuronal-specific or cell-type specific. It could be non-cell autonomous even if glia cells are not participating, if, for instance is through neuronal connections or neuronal release of some factors that affect phenotypes in a non-cell-autonomous manner.

Is the rationale for developing the new method (or application) clearly explained?

Yes

Is the description of the method technically sound?

Yes

Are sufficient details provided to allow replication of the method development and its use by others?

Yes

If any results are presented, are all the source data underlying the results available to ensure full reproducibility?

Yes

Are the conclusions about the method and its performance adequately supported by the findings presented in the article?

Yes

Competing Interests: No competing interests were disclosed.

Reviewer Expertise: Developmental Neuroscience

I confirm that I have read this submission and believe that I have an appropriate level of expertise to confirm that it is of an acceptable scientific standard.

Reviewer Report 11 March 2020

<https://doi.org/10.21956/wellcomeopenres.17119.r37774>

© 2020 Vemuri M. This is an open access peer review report distributed under the terms of the [Creative Commons Attribution License](#), which permits unrestricted use, distribution, and reproduction in any medium, provided the original work is properly cited.



Mohan C. Vemuri

Thermo Fisher Scientific, Frederick, MD, USA

The paper describes an in vitro human neuronal culture system for the study of calcium signaling in normal and patients with any brain disorders. These cultures can be extended up to 120 days in a culture dish - which is a huge advantage to researchers.

The description of the method for others to follow and repeat is well laid.

Methodology of neural differentiation, characterization with specific NSC and NPC and non-neural cell markers and transcriptome analysis to pin point the cluster of genes that are likely impacted is done in an exceptionally nice and convincing way.

Few questions:

1. Should Sox1 staining not be generally nuclear? I see it looks more cytoplasmic.
2. This study is conducted with only XCL1 neural stem cells from commercial sources. Although its nice and good, it would have been better to include a disease based NSC (commercial or developed institutionally) and validate these methods for disease paradigms.

Authors - please do not consider this comment of mine as negative.

I really commend the authors and investigators to develop this robust method that will be useful for all global researchers.

Is the rationale for developing the new method (or application) clearly explained?

Yes

Is the description of the method technically sound?

Yes

Are sufficient details provided to allow replication of the method development and its use by others?

Yes

If any results are presented, are all the source data underlying the results available to ensure full reproducibility?

Yes

Are the conclusions about the method and its performance adequately supported by the findings presented in the article?

Yes

Competing Interests: No competing interests were disclosed.

Reviewer Expertise: My areas of research include iPSC and their differentiation towards Neural and Immune cell types of cell therapy relevance. I head the division of cell and gene therapy that comprises the cell therapy modeling, isolation of cell therapy suitable cells from human origin.

I confirm that I have read this submission and believe that I have an appropriate level of expertise to confirm that it is of an acceptable scientific standard.
